DEVELOPMENT OF CONTROLLER FOR AN UNDERACTUATED AUTONOMOUS UNDERWATER VEHICLE (AUV)

DR. MAZIYAH MAT NOH
DR. ZAINAH MD ZAIN
DR. NORMANIHA ABD. GHANI
DR. YASMIN ABDUL WAHAB
DR. AKHTAR RAZUL RAZALI

RESEARCH VOT NO:

RDU1703134

Faculty of Electrical & Electronics Engineering

UNIVERSITI MALAYSIA PAHANG

2019

ACKNOWLEDGEMENTS

First of all, thanks to Allah SWT on His blessing to make this research successful. Million thankful and appreciation to all research mates, whose encouragement, guidance and support from the initial to the final level with patience and knowledge enabled this group to develop an understanding of the project. The invaluable guidance and advice in this project has been a source of inspiration through the course of this research.

Finally, we would also like to express our sincere grateful to all our friends and students of Faculty of Electrical & Electronics Engineering for their helping during the time in need and who had directly or indirectly contributed in one way or another towards to accomplish of this project. Last but not least, thank you to all that always supported us in any respect during the completion of the project.

ABSTRAK

Pengawalan pergerakkan kenderaan bawah air berautonomi (AUV) amat penting bagi memperolehi data yang tepat terutama dalam persekitaran bawah air mempunyai ketidaklelurusan yang tinggi dan gangguan bawah air serta kerumitan dalam model. Peluncur bawah air berautonomi (AUG) yang merupakan sejenis AUV yang mempunyai penggerak yang terhad. Atas sebab ini, objektif utama penyelidikan ini adalah untuk membina hukum kawalan yang mempunyai keupayaan dalam menghadapi gangguan luar dan ketidakpastian akibat pekali hidrodinamik. Oleh itu, pengawal tegar tak lelurus telah direka dengan menggunakan algoritma pengawal kawalan mod gelangsar piuhan lampau langkah mengundur (BSTSMC) untuk model tak lelurus bagi satah membujur AUG. BSTSMC telah diuji dengan gangguan luar dan perubahan parameter. Penanda aras BSTSMC telah dibuat dengan strategi-strategi pengawal mod gelangsar yang lain bagi melihat prestasinya dalam penindasan kadar gelatuk. BSTSMC telah ditanda aras dengan pengawal mod gelangsar piuhan lampau (STSMC), pengawal mod gelangsar langkah mengundur (BSMC).Hasil simulasi telah menunjukkan bahawa pengawal yang dicadangkan menghasilkan kadar gelatuk terkecil lebih kurang 1000 kali lebih kecil daripada STSMC dan 100 kali lebih kecil daripada langkah mengundur SMC dalam kes namaan, kes gangguan luar dan kes perubahan parameter. Ralat keadaan mantap bagi pengawal yang dicadangkan ini juga menghasilkan ralat keadaan mantap terkecil iaitu empat kali lebih kecil daripada STSMC dan langkah mengundur SMC dalam semua kes untuk sudut anggul dan 100 kali lebih kecil daripada STSMC dan 100 langkah mengundur. Pengawal yang dicadangkan adalah merupakan kaedah penindasan gelantuk yang baharu yang menghasilkan ralat keadaan mantap terkecil dan gelantuk telah ditindaskan dalam semua kes.

ABSTRACT

The autonomous underwater glider (AUG) demonstrates highly nonlinear and complexity in its dynamic model and also coupled with external underwater environment and disturbance. With limited actuators, the only option that AUG has in facing such environment and disturbances is by using strategies of control algorithm. For this reason, the main objective of this research is to formulate the control law that has the capability in facing the external disturbances and uncertainties due its hydrodynamics coefficients. As a result, a robust and reliable has been designed using back-stepping super twisting sliding mode control algorithm (BSTSMC) for nonlinear model of longitudinal plane of an AUG. The BSTSMC was tested for external disturbance and parameter variations. The BSTSMC has been benchmarked its performances with other sliding mode control (SMC) strategies to evaluate the chattering suppression of the controllers. The BSTSMC was benchmarked with super twisting SMC (STSMC) and back-stepping SMC. The simulation results have shown that the proposed controller provides the smallest chattering about more than 1000 times smaller than STSMC, more than 100 times smaller than back-stepping SMC in nominal, disturbance and parameter variation cases respectively. The steady error of the proposed controller also gives the smallest steady state error of four times smaller than STSMC and back-stepping SMC in all cases for pitching angle and 100 times smaller than STSMC and back-stepping for excess mass. The proposed controller is a new chattering suppression method which provides the smallest steady state error and chattering has been also suppressed in all cases.

TABLE OF CONTENT

LIST OF TABLES

LIST OF FIGURES

LIST OF SYMBOLS

α	Angle of attack
m_b	Ballast point mass
u_b	Ballast pumping rate
D	Drag
C_D, C_{DO}	Drag coefficients
m_{em}	Excess mass (net buoyancy) of AUG
m_w	Fixed point mass
g	Gravitational acceleration
v_3	Heave
m_h	Hull mass
J_1, J_2, J_3	Inertia of AUG
m_i	ith diagonal element of total mass
u_i	ith control law for BSTSMC
u_{i1}	ith discontinuous control law for BSTSMC
s_i	ith sliding surface
δ_k	kth bounded matched perturbation
e_k	kth tracking error
ρ_k	kth upper bounded matched perturbation
$K_{\omega_2^1}, K_{\omega_2^2}$	Linear and nonlinear quadratic damping constant coefficients
m_p	Internal moving mass of AUG
L	Lift
C_L, C_{LO}	Lift coefficients
C_M, C_{MO}	Moment coefficients
w_{10}, w_{20}	Nominal control law for BISTSMC application in AUG
ω_2	Pitch rate (AUG)
θ	Pitching angle
M_{DL2}	Pitching moment
ω_1	Roll angle
R	Rotation matrix
α_1	Stabilising function for BSTSMC
β	Sideslip angle
P_p	Momentum of internal movable mass

P_{p1}	Momentum of internal movable mass in x-axis
P_{p3}	Momentum of internal movable mass in z-axis
v_1	Surge
r_b	Vector of ballast point mass
r_p	Vector of internal movable mass
r_{p1}	Vector of internal movable in x-axis
r_{p3}	Vector internal movable mass in z-axis
ω_3	Yaw angle

LIST OF ABBREVIATIONS

2D	Two-Dimensional
3D	Three-Dimensional
AUG	Autonomous Underwater Glider
AUV	Autonomous Underwater Vehicle
BSMC	Back-stepping Sliding Mode Control
BSTSMC	Back-stepping Super twisting Sliding Mode Control
CB	Centre of Buoyancy
CG	Centre of Gravity
CFD	Computational Fluid Dynamic
DOF	Degree-of-Freedom
DSMC	Dynamic Sliding Mode Control
EAVE	Experimental Autonomous Underwater Vehicle
EOM	Equation of Motion
FLC	Fuzzy Logic Control
GA	Genetic Algorithm
HOSMC	Higher Order Sliding Mode Control
ISMC	Integral Sliding Mode Control
ISTSMC	Integral Super twisting Sliding Mode Control
LQR	Linear-Quadratic Regulator
MMS	Marine Systems Simulator
MPC	Model Predictive Control
NDRE	Norwegian Defence Research Establishment
NN	Neural Network
NDO	Nonlinear Disturbance Observer
PD	Proportional-Derivative
PI	Proportional Integral
PID	Proportional-Integral-Derivative
PSO	Part Swarm Optimisation
REMUS	Remote Environmental Monitoring Units
RMSE	Root Mean Square Error
ROV	Remotely Operated Vehicle
SIFLC	Single Input Fuzzy Logic Controller
SISO	Single-Input-Single-Output
SMC	Sliding Mode Control

SMCB	SMC based on boundary layer
SMCS	SMC based on saturation function
SONCS	Self-Organizing Neural-net Control System
SOSMC	Second Oeder Sliding Mode Control
SPURV	Self-Propelled Underwater Research Vehicle
STSMC	Super twisting Sliding Mode Control
UARS	Unmanned Arctic Research Submersible
UV	Underwater Vehicle
UUV	Unmanned Underwater Vehicle
WHOI	Woods Hole Oceanography Institute

CHAPTER 1

INTRODUCTION

1.1 Background

The underwater robotic researches have received great attention since the past three decades. The robotic technologies have helped the researchers in expanding the scientific underwater exploration such as scientific ocean exploration, surveillance, commercial inspection of undersea facilities and military operations. Generally, underwater vehicle (UV) is divided in two main categories which are manned and unmanned underwater vehicles (UUVs). The UUV is further divided into remote operated vehicles (ROVs) and autonomous underwater vehicles (AUVs). The classification of UVs is summarised in Figure 1-1. The autonomous underwater glider (AUG) is considered as a special class of AUVs.

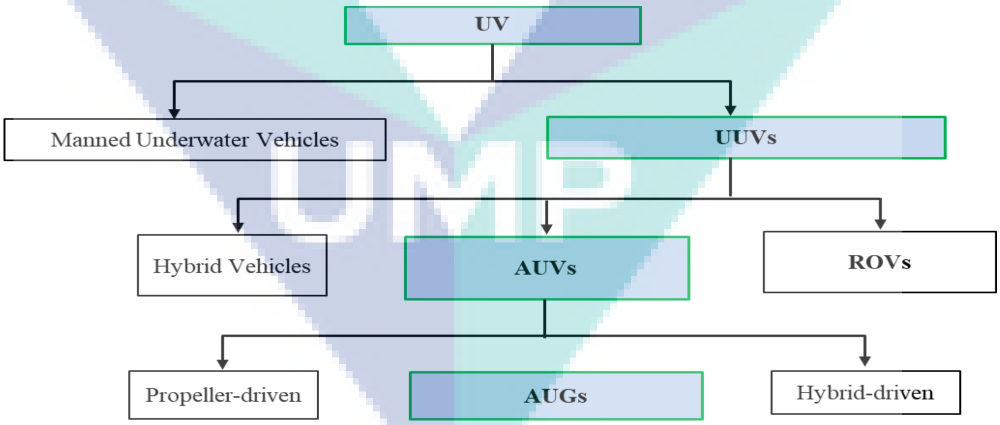

Figure 1-1 The classification of underwater vehicles (Md Zain, 2012)

The underwater glider was inspired by Henry Stommel (1989), called Slocum float. A decade later, three operational gliders namely Slocum (Webb et al., 2001), Spray (Sherman et al., 2001) and Seaglider (Eriksen et al., 2001) were developed and tested, and their performance was proven.

The basic design of the AUG is buoyancy-driven with fixed wings and rudder, internal masses and a ballast pump. The AUG glides through the water column by shifting the internal movable mass in translational or rotational depending on the design of the movable tracks and pumping of the ballast pump. By doing these, the pitching angle and the depth can be controlled and cause the AUG to glide in saw-tooth pattern. Figure 1-2 shows the ideal gliding of a buoyancy-driven AUG.

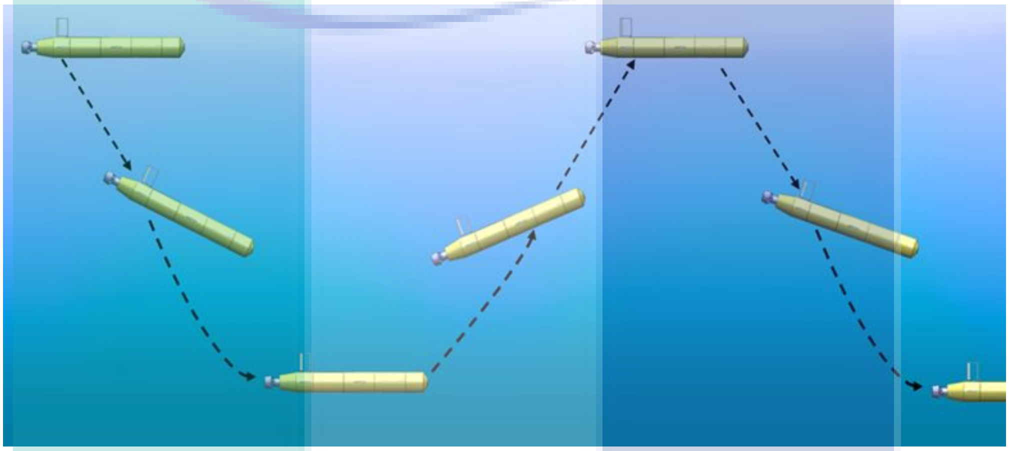

Figure 1-2 Gliding motion of AUG (Isa, 2015)

There are many control techniques either classical control or modern control have been employed to control AUVs and AUGs beginning from the simple proportional-integral-derivative (PID), linear-quadratic-regulator (LQR), robust control approach, adaptive control up to intelligent control such as fuzzy logic and neural network (NN). Among all the controllers, PID and LQR are widely used to control the existing gliders motion and attitude.

The sliding mode control (SMC) is one of the candidates that can be considered to improve the tracking performance of the parameters under study (control). Although the conventional SMC has suffered internally with chattering issues, however when the chattering phenomena is remedied, then the SMC is able to handle the parameter variation issue and offer the robustness towards external disturbances and uncertainties which are proven through many applications in many other systems (Jalani et al., 2010; Rhif, 2012; Li et al., 2013; Ismail et al., 2015; Heng et al., 2017; Tayebi-haghighi, 2018). In this study the chattering phenomena is reduced through integration of back-stepping and super twisting SMC (STSMC) approach.

1.2 Problem Statement

The AUG is considered as an under-actuated system with high nonlinearity of dynamics, with uncertainties in hydrodynamic coefficients and with the presence of underwater disturbance (J. Yuh, 2000; Pan & Xin, 2012). Therefore, a robust nonlinear controller algorithm is required to maintain the overall performance of the AUG.

Previous researchers have proposed and implemented various control techniques to control AUVs and AUGs. The performance of the controllers degrades with the changes. Therefore, it is highly desirable to design a controller that is able to reject perturbations due to plant uncertainties and external disturbances.

1.3 Research Objectives

This study embarks on the following objectives:

1) To formulate the mathematical model of AUG system
2) To design and apply to proposed controller in AUG system
3) To benchmark the algorithms performances by comparing the rate of chattering reduction of this proposed work towards disturbance rejection and parameter variations with other family of SMC strategies.

CHAPTER 2

LITERATURE REVIEW

2.1 Introduction

For UVs to manoeuvre autonomously, the control algorithm must be robust against perturbations and parameter variations. It is known that the UVs are difficult to control since their system is highly nonlinear and the dynamics of the vehicles are time-varying. The hydrodynamics coefficients are uncertain, mostly disturbed by water current and also changes in centre of buoyancy (CB) and centre of gravity (CG) due to the internal actuators (Budiyono, 2009; Yuh, 2000). There have been various control techniques proposed to control the AUVs and AUGs. The control techniques to control the AUVs and AUGs are divided into three main categories; linear control, nonlinear control and intelligent control strategies. This section covers the literatures of SMC applications to cover wide spectrum of literatures.

2.2 Linear Control Strategies

Linear control is used when the model of the plant is linearised about the equilibrium. In underwater vehicle, the linear control is dominated by the proportional-integral-derivative (PID) and linear quadratic regulator (LQR).

The first implementation of PID in AUVs was proposed by Chellabi & Nahon (1993). Nonlinear dynamics of the AUV were linearised and decoupled into six SISO second-order subsystems. A combined strategy of a proportional-derivative (PD) controller and LQR was proposed for the six SISO subsystems. The PD control law was designed to stabilise the system and LQR was used to cater the optimal error correcting term for improving the robustness of the PD controller. Following this first implementation, Jalving (1994) proposed a PID controller for Norwegian Defence

Research Establishment (NDRE) AUV. The nonlinear dynamics were linearised and decoupled into three subsystems which were speed, steering and diving subsystems. The speed subsystem was controlled using PI control law and this PD control law was utilised to control heading and depth. In the unmanned underwater test vehicle, Lee et al. (2009) proposed a PID controller for Manta-type unmanned underwater test vehicle to control steering and diving based on linearised model. In 2010, Santhakumar & Asokan (2010) proposed a self-tuning PID to enhance the performance of the original PID. In this work, Taguchi's method was used to build the self-tuning PID algorithm. The self-tuning performance was compared with tuning method proposed by Ziegler-Nichols. Other than these, in 2014, Watson & Green (2014) proposed a PID for micro AUV to control depth. The continuous PID was discretised using Tustin approximation to compute the discrete version of PID controller. Recently, Mohd Aras et al (2017) proposed PID controller to control heading. The PID controller is usually designed using the standard block available in MATLAB/SIMULINK and thus the gains are tuned using auto tune command. However, the proposed PID is sensitive to uncertainties and external disturbances.

Leonard & Graver (2001) designed the LQR for the ROGUE AUG. The LQR was designed for steady glides of 30° and 45° downward and upward. There was no significant tuning performed to optimise the controller parameters. Joo & Qu (2015) designed LQR to control the motion of a hybrid AUV. The LQR performance was tested for steady glide of 30° downward and upward. In the same year, Javaid et al. (2015) designed the LQR to control the longitudinal plane of the AUG. The LQR was simulated for two different wing designs which were tapered shape and rectangular shape to observe the behaviour of the glider motion with different shape of wing. A year after that, Tchillian et al (2016) also proposed the LQR for the longitudinal plane of an AUG.

As conclusion, the linear controllers provide good tracking performances. However, since the model is linearised about the equilibrium point, the performance of the controller is only effective in a small neighbourhood of the equilibrium.

2.3 Nonlinear Control Strategies

Most of the systems are nonlinear. The nonlinear control strategies offer a better option in handling the nonlinearities, uncertainties, disturbances and changes in parameters in which linear control strategy is unable to handle. There are various nonlinear controls have been implemented in AUVs and AUGs such as SMC, back-stepping control and adaptive control.

The SMC strategy is known for its robustness against perturbations such as parameter variations and external disturbances. Since the UVs are highly nonlinear with time variant dynamics, thus it is found in many research works in which the SMC technique was employed. The main drawback of the SMC is chattering phenomena that is induced by high frequency switching of the discontinuous control. However, many approaches can be used to reduce the chattering phenomena.

The first implementation of SMC in AUVs was found in 1985 by Yoerger & Slotine (1985). In this research, the boundary layer SMC control law was developed for the Experimental Autonomous Vehicle (EAVE) and this control law was only developed for the nonlinear model for the horizontal plane. Dougherty et al. (1988) proposed the conventional SMC that employed the signum function in discontinuous control. The controller was designed for hovering control of an AUV. Later, Healey & Lienard (1993) implemented SMC to control speed, heading and depth. The controller was designed based on decoupled subsystems which were speed, steering and diving subsystems. They employed the hyperbolic tangent smooth function to replace the signum function. Wang et al. (2002) employed the basic SMC which its signum function was employed in the discontinuous control for 5 DOF nonlinear system that controlled surge, sway, heave, pitching and yaw of a ZHISHUI-III AUV. In 2015, Kim et al. (2015) employed integral sliding mode control ISMC to reduce chattering. ISMC is also known as no reaching phase SMC until now since the algorithm ensures that the sliding begins at time, $t = 0$. In addition, Kim et al. (2015) had also developed controller control depth of Cyclops AUV.

Salgado-Jimenez & Jouvencel (2003) employed higher order sliding mode known as the twisting SMC and super twisting SMC (STSMC) for depth control of a TAIPAN AUV. The performances of both controllers were compared with PD controller. Khan et al. (2012) compared the performance of the conventional SMC, terminal SMC (TSMC) and STSMC. The controllers were designed to control the lateral dynamics of an AUV. Ruiz-duarte and Loukianov (2015) proposed the super twisting SMC to control depth of the AUV. The performance of the STSMC was compared to the nonlinear observer in term of robustness against external disturbance and parameter variations.

The back-stepping is another technique used to control the motion of the AUVs and AUGs. The back-stepping is known as a recursive systematic design methodology. It uses Lyapunov stability theorem to analyse the stability of the controller. The basic idea of back-stepping is the design that breaks up into sequence of the sub-problems of the lower order of the system and then recursively uses the states as “virtual controls” to attain the intermediate control laws using the Lyapunov function.

Caiti & Calabro (2010) proposed the integral back-stepping technique with fuzzy to improve the adaptation of the controller to hydrodynamics uncertainties and external disturbances. The controller was designed for the FOLAGA AUV. Ferreira et al (2011) proposed the back-stepping control to the MARES AUV in the presence of thruster fault. Two control laws were derived to control the pitching angle and the depth of MARES AUV. Wei et al. (2015) researched on the back-stepping control based on nonlinear disturbance observer (NDO) to control the depth of the AUV. The NDO is commonly used to estimate the disturbance. In Cervantes et al (2016), the output based back-stepping was proposed to control the linear position and yaw angle of the AUV. The algorithm of this work combined the back-stepping like form and a robust exact differentiator. The simulation results proved that the proposed controller provided an acceptable performance. Recently Rath et al (2017) proposed the back-stepping control for diving and steering planes of an AUV. The control laws for diving and steering planes were designed separately. However, the proposed controller was not tested in the system with the presence of uncertainties. For AUG, several works based on back-stepping control were reported in (Burlion et al., , 2004; Caiti et al., 2012; Cao et al., 2015; Cao et al, 2016).

In Antonelli et al. (2001), the adaptive control was designed to control the six degree of freedom (DOF) of ODIN ROV and AUV that combined SMC with an adaptive controller system parameter estimation. Later, Antonelli (2007) presented the adaptive control to control 6 DOFs of ODIN and AUV. However, in this work, the adaptive controller was a combination of PD with an adaptive/integral compensator to compensate the persistent dynamic effects such as the restoring forces and the ocean currents. In 2014, Sahu & Subudhi (2014) designed the adaptive controller to control the liner position and yaw angle of AUV. The adaptive control was combined with PD controller which was able to adapt the uncertainties in hydrodynamic parameters. One year later, Barbalata et al. (2015) proposed the adaptive control method to control the 4 DOFs of AUV. The adaptive control was used to determine the gain of the PD controller online basis through position/velocity error.

In general, the nonlinear control provides high robustness against nonlinear dynamics, uncertainties in hydrodynamic and environment disturbances. Many applications that are used nowadays usually combine two methods of control approach to enhance a single approach. However, the combination of back-stepping and sliding mode control application in AUG is still open for implementation.

2.4 Intelligent Control Strategies

There are several categories of control algorithms fall under intelligent control. The NN and fuzzy logic controls (FLCs) are the most prominent controls employed for controlling the motion of the underwater vehicles. The advantage of intelligent control is its ability to adapt and robustness to the nature of highly nonlinear and dynamic environment of the underwater vehicles.

Various researches have been done previously using NN as a backbone to control the AUVs. In 2010, Amin et al. (2010) introduced two online learning methods which were an online multilayer perceptron NN (OMLPNN) and online recurrent multilayer perceptron NN (OMLPNN) to control a testbed NPS AUV. The controllers were designed to compute the forces and moments of the AUV so that the tracking error could be eliminated and the inverse model of AUV could be generated in which also determined the speed of the propeller angles of control surface. García-Córdova and Guerrero-González (2011) proposed a biologically-inspired NN for trajectory tracking of AUVs. The Self-Organisation Direction Mapping Network (SODMN) which was an unsupervised kinematic adaptive NN controller was designed for guiding an AUV towards a target in a 3D workspace. The angular velocity of each propeller was selected in order to control the motion of the AUV. The AUV motions were controlled by selecting the angular velocity of each propeller. Eski & Yildirim (2014) designed robust controller based on NN for linear model of AUV. The NN was designed based on resilient back-propagation structure to adjust the weights of the NN. The performance of the proposed control was compared to the PID controller. Recently Guo et al. (2017) proposed the adaptive NNs with control input nonlinearities using reinforcement learning to control fully actuated AUV. The reinforcement learning was used to optimise the tracking capability in presence of nonlinearities and disturbances. The controller was designed based on AUV discrete model. The performance of the proposed controller was compared to general NN and PD controllers. The FLC is another prominent intelligent control algorithm used to control UVs. The FLC is a rule-based control in which the control analyses the system based on logical variables between true (1) or false (0).

The ability of FLC to approximate the nonlinear mapping of the system from input to output, makes it suitable for nonlinear control (Zhao & Yuh, 2005). The satisfactory performance of the FLC can be achieved by defining the correct fuzzification and membership functions. Nevertheless, the experimental data is needed for defining the correct fuzzification of the membership functions and fuzzy rules and thus increasing the computational time. Ishaque et al. (2010) and Amjad et al. (2010) proposed a Single Input Fuzzy Logic Controller (SIFLC). This controller was simulated using Marine System Simulator (MSS). It has reduced tuning effort and computational time in the orders of two magnitudes than the conventional FLC. The FLC type Sugeno model was proposed by Lee & Kang (1998). It was implemented in underwater vehicle by taking into account the influence thruster dynamic. In terms of system algorithm, the research made by Gua & Huang (1996) proposed an algorithm that combined the genetic algorithm (GA) and FLC to control the AUVs. The GA was used to optimise the membership function. The fitness functions were designed such that the rise time, maximum overshoot and steady state error are satisfied.

In general, the intelligent control offers very good tracking performance and adaptability to hydrodynamics uncertainties and environmental disturbances. However, it usually suffers from the computational time during the tuning process and the parameter estimation process (Zhao & Yuh, 2005).

CHAPTER 3

METHODOLOGY

3.1 Introduction

This chapter presents the modelling of the AUG system and design of control algorithm. The process of establishing the nonlinear model will be explained in Section 3.2. The controller for nonlinear system was designed based on the SMC and back-stepping control strategies that has been named as back-stepping super twisting sliding mode control algorithm (BSTSMC) is explained in Section **Error! Reference source not found.**. The performance of the proposed is benchmarked with other SMC families where the algorithms are explained in Section **Error! Reference source not found.** and 3.3.3 respectively.

3.2 Nonlinear model of AUG for longitudinal plane

The mathematical model of longitudinal plane of AUG is based on the model that was proposed by Graver (2005). The model was proposed with assumption that the internal movable mass moved along x and z axes. However, in this work, the movable mass moved along x-axis only. Two reference frames of the glider are defined and the initial frame (i-frame) and the body frame (b-frame) are shown in Figure 3-1. The initial frame is assumed to be non-rotating (fixed) frame. The body frame is fixed to the glider's body with its origin is at CB. The body axes are specified as X, Y, and Z which lay along x-axis, y-axis and z-axis respectively. The notations of the overall AUG model are specified in **Error! Reference source not found.**. The CG is assumed to coincide with CB.

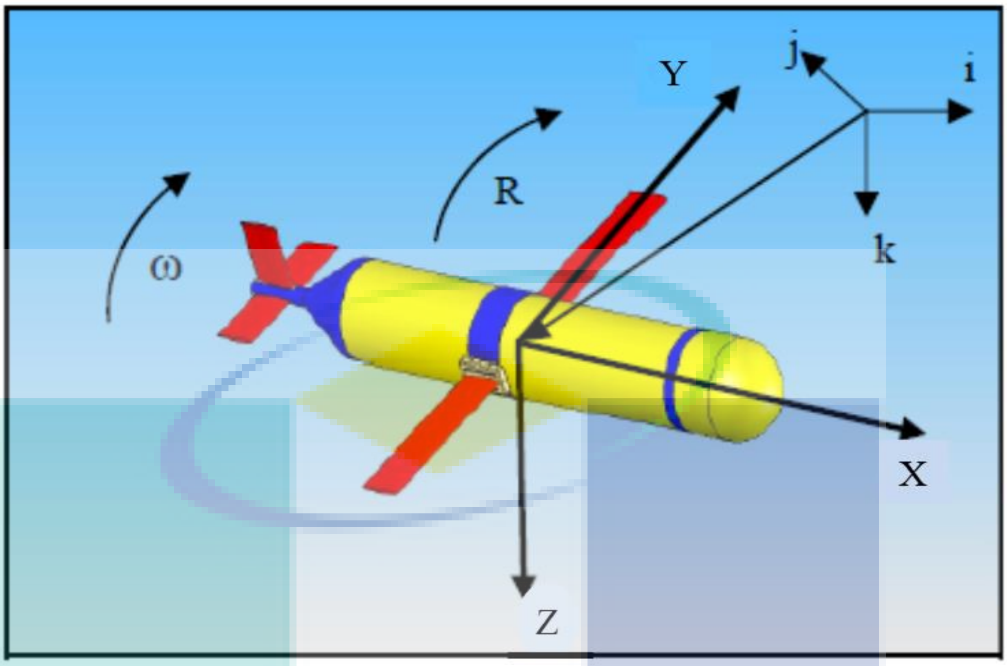

Figure 3-1 The reference frame of the glider

Table 3-1 The notations of the AUG

	Linear and angular velocity	Position and orientation
Motion in the x-direction (surge)	v_1 (m/s)	x
Motion in the y-direction (sway)	v_2 (m/s)	y
Motion in the z-direction (heave)	v_3 (m/s)	z
Rotation about the x-axis (roll)	ω_1 (rad/s)	ϕ
Rotation about the y-axis (pitching)	ω_2 (rad/s)	θ
Rotation about the z-axis (yaw)	ω_3 (rad/s)	ψ

The longitudinal model based on Graver (2005) is presented in this sub-chapter. The detail derivation of Graver's work can be found in Graver et al. (1998) and Leonard & Graver (2001). The following assumptions have been made to reduce the complexity of the model without jeopardising the overall performance of the glider.

i) The offset static mass, mw was set to zero ($m_w = 0$)

ii) The ballast point mass was fixed at the centroid of the glider body ($r_b = 0$).

The assumptions have caused the glider to be in its simplified internal masses as shown in Figure 3-2. The assumptions also eliminated the coupling due to offset static mass, and the coupling between the ballast and the glider inertia and the pitching moment.

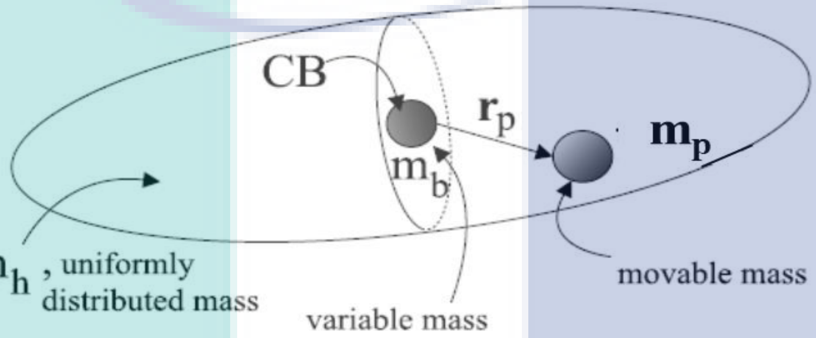

Figure 3-2 The simplified internal masses of the glider (Graver, 2005)

The longitudinal plane model was established by setting all the parameters related to lateral to zero, lateral position (y), lateral velocity (v_2), roll rate (ω_1) and yaw rate (ω_3) as shown in the matrices form below.

Rotation matrix:

$$R = \begin{bmatrix} \boldsymbol{cos\theta} & \mathbf{0} & \boldsymbol{sin\theta} \\ \mathbf{0} & \mathbf{1} & \mathbf{0} \\ \boldsymbol{-sin\theta} & \mathbf{0} & \boldsymbol{cos\theta} \end{bmatrix} \quad \text{3-1}$$

Body position:

$$\boldsymbol{b} = \begin{bmatrix} x \\ 0 \\ z \end{bmatrix} \quad \text{3-2}$$

Linear velocity:

$$\boldsymbol{v} = \begin{bmatrix} v_1 \\ 0 \\ v_3 \end{bmatrix} \quad 3\text{-}3$$

Angular velocity:

$$\boldsymbol{\omega} = \begin{bmatrix} 0 \\ \omega_2 \\ 0 \end{bmatrix} \quad 3\text{-}4$$

Internal movable position:

$$\boldsymbol{r_p} = \begin{bmatrix} \boldsymbol{r_{p1}} \\ \boldsymbol{0} \\ \boldsymbol{r_{p3}} \end{bmatrix} \quad 3\text{-}5$$

Internal movable mass momentum:

$$\boldsymbol{P_p} = \begin{bmatrix} \boldsymbol{P_{p1}} \\ \boldsymbol{0} \\ \boldsymbol{P_{p3}} \end{bmatrix} \quad 3\text{-}6$$

Control input:

$$\boldsymbol{u} = \begin{bmatrix} \boldsymbol{u_{aug1}} \\ \boldsymbol{0} \\ \boldsymbol{u_{aug3}} \end{bmatrix} \quad 3\text{-}7$$

The above setup has produced the equation of motion (EOM) for the longitudinal plane as written in Equation (3-8) – (3-18).

$$\dot{x} = v_1 \cos(\theta) + v_3 \sin(\theta) \quad 3\text{-}8$$

$$\dot{z} = -v_1 \sin(\theta) + v_3 \cos(\theta) \quad 3\text{-}9$$

$$\dot{\theta} = \omega_2 \quad 3\text{-}10$$

$$\dot{\omega}_2 = \frac{1}{J_2}\{(m_3 - m_1)v_1v_3 - (r_{p1}P_{p1}\omega_2 + r_{p3}P_{p3})\omega_2 - m_p g\big(r_{p1}\cos(\theta) + r_{p3}\sin(\theta)\big) + M_{DL2} - r_{p3}u_{aug1} + r_{p1}u_{aug3}\} \quad 3\text{-}11$$

$$\dot{v}_1 = \frac{1}{m_1}\{-m_3v_3\omega_2 - P_{p3}\omega_2 - m_{em}g\sin(\theta) + L\sin(\alpha) - D\cos(\alpha) - u_{aug1}\} \quad 3\text{-}12$$

$$\dot{v}_3 = \frac{1}{m_3}\{m_1v_1\omega_2 + P_{p1}\omega_2 + m_{em}g\cos(\theta) - L\cos(\alpha) - D\sin(\alpha) - u_{aug3}\} \quad 3\text{-}13$$

$$\dot{r}_{p1} = \frac{1}{m_p}P_{p1} - v_1 - r_{p3}\omega_2 \quad 3\text{-}14$$

$$\dot{r}_{p3} = \frac{1}{m_p}P_{p3} - v_3 + r_{p1}\omega_2 \quad 3\text{-}15$$

$$\dot{P}_{p1} = u_{aug1} \quad 3\text{-}16$$

$$\dot{P}_{p3} = u_{aug3} \quad 3\text{-}17$$

$$\dot{m}_b = u_b \quad 3\text{-}18$$

where m_{em} is the net buoyancy, m_1, and m_3 denote the first and third element of total mass, D and L, and M_{DL2} represents the drag, lift and pitching moment of the hydrodynamic force and moment. They were defined by Graver (2005) as

$$m_{em} = m_h + m_p + m_b - m_{df} \quad 3\text{-}19$$

$$L = (C_{LO} + C_L\alpha)(v_1^2 + v_3^2) \quad 3\text{-}20$$

$$D = (C_{DO} + C_D\alpha^2)(v_1^2 + v_3^2) \quad 3\text{-}21$$

$$M_{DL2} = (C_{MO} + C_M\alpha)(v_1^2 + v_3^2) + K_{\omega_2^1}\omega_2 + K_{\omega_2^2}\omega_2^2 \quad 3\text{-}22$$

where m_h, m_p, and m_{df} are the mass of the hull, internal movable mass and displaced fluid mass respectively. α is the angle of attack. C_L, C_{LO}, C_D, C_{DO}, C_M, and C_{MO} are the hydrodynamic lift, drag and pitching moment coefficients respectively. The system and input states are defined as

$$\boldsymbol{x} = [\boldsymbol{x_1}\ \boldsymbol{x_2}\ \boldsymbol{x_3}\ \boldsymbol{x_4}\ \boldsymbol{x_5}\ \boldsymbol{x_6}\ \boldsymbol{x_7}]^{\boldsymbol{T}} = \left[\boldsymbol{\theta}\ \boldsymbol{\omega_2}\ \boldsymbol{v_1}\ \boldsymbol{v_3}\ \boldsymbol{r_{p1}}\ \dot{\boldsymbol{r}}_{\boldsymbol{p1}}\ \boldsymbol{m_b}\right]^{\boldsymbol{T}} \quad 3\text{-}23$$

$$\boldsymbol{u} = [\boldsymbol{u_1}\ \boldsymbol{u_2}]^{\boldsymbol{T}} \quad 3\text{-}24$$

3.3 Controller design

The controller for nonlinear system was designed based on the SMC and back-stepping control strategies that has been named as back-stepping super twisting sliding mode control algorithm (BSTSMC). The stability of the proposed controller was determined via Lyapunov stability theory where the gradient of the Lyapunov function must be negative definite to ensure the proposed controllers algorithm was asymptotically stable and converge in a finite time. The controller was tested in the presence of disturbance and parameter variations. The performance of the proposed controller was benchmarked with combination of back-stepping and SMC strategies for the model developed in Section 3.2. The controller of this research was designed for tracking problem. The formulation for tracking problem in the nonlinear system is established. The nonlinear equations can be written in the following form:

$$\begin{aligned} \dot{x}_1 &= x_2 \\ \dot{x}_2 &= x_3 \\ &\vdots \\ \dot{x}_k &= f_k(x,t) + g_k(x,t)u_i + g_k\delta_k(x,t) \end{aligned} \quad 3\text{-}25$$

where $x \in \Re^n$ and $u \in \Re^m$ are defined as state and input vectors respectively, $\delta_k(x,t)$ represents the bounded matched perturbations, $k = 1,2,\ldots,n$ and $i = 1,2,\ldots,m$. $\delta_k(x,t)$ is bounded with a known norm upper bound,

$$|\delta_k(x,t)| \leq |\rho_k(x,t)| \quad 3\text{-}26$$

The last equation in Equation (3-25) is rewritten in the form that is suitable for the proposed controller algorithm as written in Equation (4.3)

$$\dot{x}_k = \varphi_k(x,t) + g_k(x,t)u_i + g_k\delta_k(x,t) = \chi_i(x,u_i,t) + u_i + g_k\delta_k(x,t) \quad 3\text{-}27$$

For tracking problem, the error is defined as the deviation of the output from its desired value as stated below.

$$error = e_k = x_k - x_{kd} \quad 3\text{-}28$$

3.3.1 Back-stepping super twisting sliding mode control (BSTSMC) algorithm

The proposed controller design framework is depicted in Figure 3-3. The sliding surface is designed based on the back-stepping control strategy and the super twisting algorithm is used for discontinuous control.

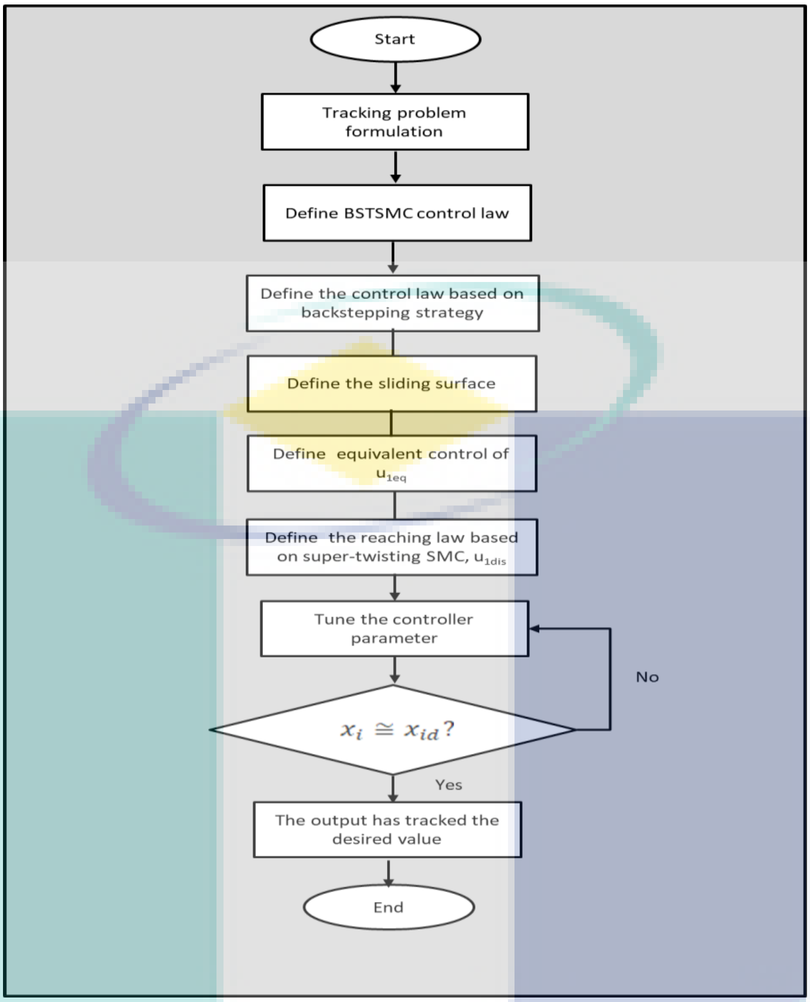

Figure 3-3 BSTSMC design flow

In this work, the pitching angle, x_1 and the net buoyancy, m_{em} are chosen as the outputs where m_{em} is indirectly controlled by the ballast mass, x_7. Therefore, in the research, two subsystems were developed in the form of Equation (3-25) to control the pitching angle, x_1 and net buoyancy via x_7 . The output state is defined in Equation (3-32).

$$y_1 = x_1 \tag{3-29}$$

$$y_2 = m_{em} = m_h + m_p + m_b - m_{df}$$

The subsystems to control x_1 and m_{em} are written in Equation (3-32) and Equation (3-34) respectively. The design procedure is shown in the following steps.

$$\dot{x}_1 = x_2 \tag{3-30}$$

$$\dot{x}_2 = f_1(x,t) - g_1(x,t)u_1 - g_1(x,t)\delta_1(x,t)$$

$$\dot{x}_7 = u_2 + \delta_5(x,t) \tag{3-31}$$

Step 1: Design of control law, to track x_1 .

i) Define the tracking error of x_1 and its time derivative

$$e_1 = x_1 - x_{1d} \tag{3-32}$$

$$\dot{e}_1 = \dot{x}_1 - \dot{x}_{1d} = x_2 - \dot{x}_{1d} \tag{3-33}$$

ii) Define the Lyapunov function (LPF) and its time derivative as

$$V_1(e_1) = \frac{1}{2}e_1^2 \tag{3-34}$$

$$\dot{V}_1(e_1) = e_1\dot{e}_1 = e_1(x_2 - \dot{x}_{1d}) \tag{3-35}$$

As x_2 is viewed as a virtual control, the desired virtual control known as stabilising function is then defined as

$$\alpha_1 = -K_{11}e_1 + \dot{x}_{1d} \quad \text{3-36}$$

where K_{11} is a positive constant. Thus, Equation (3-35) becomes

$$\dot{V}_1 = e_1(-K_{11}e_1 + \dot{x}_{1d} - \dot{x}_{1d}) = -K_{11}e_1^2 < 0 \quad \text{3-37}$$

iii) The sliding surface is defined as second error variable as in Equation (3-38)

$$s_{1bstsmc} = x_2 - \alpha_{1bstsmc} \quad \text{3-38}$$

Rearranging Equation (3-38)

$$x_2 = s_{1bstsmc} + \alpha_{1bstsmc} \quad \text{3-39}$$

and the dynamic of the sliding surface is written as in Equation (3-40) along with Equation (3-25).

$$\begin{aligned}\dot{s}_{1bstsmc} &= \dot{x}_2 - \dot{\alpha}_{1bstsmc} \\ &= f_1(x,t) - g_1(x,t)w_{1bstsmc} + g_1(x,t)\delta_1(x,t) \\ &+ K_{11btstsmc}\dot{e}_1 - \ddot{x}_{1d}\end{aligned} \quad \text{3-40}$$

The Lyapunov function and its time derivative are defined as

$$V(e_1, s_{1bstsmc}) = \frac{1}{2}(e_1^2 + s_{1bstsmc}^2) \quad \text{3-41}$$

$$\dot{V}(e_1, s_{1bstsmc}) = e_1\dot{e}_1 + s_{1bstsmc}\dot{s}_{1bstsmc} = -K_{11bstsmc}e_1^2 + s\{f_1(x,t) - g_1(x,t)u_1 + g_1(x,t)\delta_1(x,t) + e_1 + K_{11bstsmc}\dot{e}_1 - \ddot{x}_{1d})) \quad \text{3-42}$$

The equivalent control is determined when $\dot{s}_1 = 0$ as given in Equation (3-43).

$$u_{1bstsmc\_eq} = \frac{1}{g_1}\{f_1(x,t) + g_1(x,t)\delta_1(x,t) + e_1 + K_{11bstsmc}\dot{e}_1 + K_{12bstsmc}s_{1bstsmc} - \ddot{x}_{1d}\} \quad 3\text{-}43$$

iv) Define the discontinuous control $u_{1bstsmc\_dis}$

The reachability conditions of back-stepping STSMC is defined based on STSMC. The reachability condition is written in Equations (3-44).

$$u_{1bstsmc\_dis} = -\beta_{11bstsmc}|s_{1bstsmc}|^p sign(s_{1bstsmc}) - \beta_{12bstsmc}\int_0^t sign(s_{1bstsmc})\,dt \quad 3\text{-}44$$

Step 2: Design of control law, to track m_{mem}.

i) The sliding surface is defined as second error variable as in Equation (3-45)

$$s_{2bstsmc} = e_3 = x_7 - x_{7d} \quad 3\text{-}45$$

The time derivative of sliding surface is written as

$$\dot{s}_{2bstsmc} = \dot{e}_3 = \dot{x}_7 - \dot{x}_{7d} = u_{2bstsmc} - \dot{x}_{7d} + \delta_5(x,t) \quad 3\text{-}46$$

The Lyapunov function and its time derivative are defined as

$$V(s_{2bstsmc}) = \frac{1}{2}s_{2bstsmc}^2 \quad 3\text{-}47$$

$$\dot{V}(s_{2bstsmc}) = s_{2bstsmc}\dot{s}_{2bstsmc} = s_{2bstsmc}(w_{2bstsmc} - \dot{x}_{7d} + \delta_5(x,t)) \quad 3\text{-}48$$

The equivalent control is determined when $\dot{s}_2 = 0$ as given in Equation (3-49).

$$u_{2bstsmc\_eq} = -(K_{21bstsmc}s_{2bstsmc} + \delta_5(x,t) - \dot{x}_{7d}) \quad 3\text{-}49$$

ii) Define the discontinuous control $u_{2bstsmc\_dis}$

The reachability conditions of back-stepping STSMC is defined based on STSMC. The reachability condition is written in Equations (3-50).

$$u_{2bstsmc\_dis} = -\beta_{21bstsmc}|s_{2bstsmc}|^p sign(s_{2bstsmc}) - \beta_{22bstsmc}\int_0^t sign(s_{2bstsmc})\, dt \quad 3\text{-}50$$

Finally, the control laws of back-stepping STSMC are written in Equations (3-51) and (3-52).

$$u_{1bstsmc} = \frac{1}{g_1}\{f_1(x,t) + g_1(x,t)\delta_1(x,t) + e_1 + K_{11bstsmc}\dot{e}_1 + K_{12bstsmc}s_1 - \ddot{x}_{1d}\} - \beta_{11bstsmc}|s_{1bstsmc}|^p sign(s_{1bstsmc}) - \beta_{12bstsmc}\int_0^t sign(s_{1bstsmc})\, dt \quad 3\text{-}51$$

$$u_{2bstsmc} = -(K_{21bstsmc}s_2 + \delta_5(x,t) - \dot{x}_{7d}) - \beta_{21bstsmc}|s_{2bstsmc}|^p sign(s_{2bstsmc}) - \beta_{22bstsmc}\int_0^t sign(s_{2bstsmc})\, dt \quad 3\text{-}52$$

3.3.2 Super Twisting Sliding Mode Control (STSMC) design

The STSMC is an algorithm that was introduced by Levant, (1993). This algorithm is also known as model free SMC because it only contains the discontinuous control part and the control law is free from system parameters. However, in this section the STSMC is designed using conventional SMC where the equivalent control law is derived from. Then, the discontinuous control law is designed using on super twisting algorithm. Therefore, the control law for tracking the pitching angle and net buoyancy are written in Equations (3-53) and (3-54) respectively.

$$u_{1stsmc} = u_{1stsmc\_eq} + u_{1stsmc\_dis} \quad \text{3-53}$$

$$u_{2stsmc} = u_{2stsmc\_eq} + u_{2stsmc\_dis} \quad \text{3-54}$$

The sliding surfaces and their derivatives are defined for tracking pitching angle and net buoyancy are as written in Equation (3-55), (3-56), (3-57) and (3-58).

$$s_{1stsmc} = c_{1stsmc}e_1 + \dot{e}_1 \quad \text{3-55}$$

$$s_{2stsmc} = e_3 \quad \text{3-56}$$

$$\dot{s}_{1stsmc} = c_{1stsmc}\dot{e}_1 + \dot{e}_2 \quad \text{3-57}$$

$$\dot{s}_{2stsmc} = \dot{e}_3 \quad \text{3-58}$$

The equivalent control laws are defined as $\dot{s}_{1stsmc} = 0$ and $\dot{s}_{2stsmc} = 0$

$$u_{1stsmc\_eq} = \frac{1}{g_1}\{f_1 + g_1 d_1 + c_{1stsmc}\dot{e}_1 - \ddot{x}_{1d}) \quad \text{3-59}$$

$$u_{2stsmc\_eq} = -d_5 \quad \text{3-60}$$

The reachability conditions are chosen as STSMC

$$u_{1stsmc\_dis} = -\beta_{11stsmc}|s_{1stsmc}|^p sign(s_{1stsmc}) - \beta_{12stsmc}\int_0^t sign(s_{1stsmc})dt \quad \text{3-61}$$

$$u_{2stsmc\_dis} = -\beta_{21stsmc}|s_{2stsmc}|^p sign(s_{2stsmc}) - \beta_{22stsmc}\int_0^t sign(s_{2stsmc})dt \quad \text{3-62}$$

Finally, the control laws are written in Equations (4.108) and (4.109).

$$u_{1stsmc} = u_{1stsmc\_eq} + u_{1stsmc\_dis} = \frac{1}{g_1}\{f_1 + g_1 d_1 + c_{1stsmc}\dot{e}_1 - \ddot{x}_{1d}) - \beta_{11stsmc}|s_{1stsmc}|^p sign(s_{1stsmc}) - \beta_{12stsmc}\int_0^t sign(s_{1stsmc})dt \quad 3\text{-}63$$

$$u_{2stsmc} = u_{2stsmc\_eq} + u_{2stsmc\_dis} = -d_5 - \beta_{21stsmc}|s_{2stsmc}|^p sign(s_{2stsmc}) - \beta_{22stsmc}\int_0^t sign(s_{2stsmc})dt \quad 3\text{-}64$$

3.3.3 Back-stepping Sliding Mode Control (BSMC) design

In this section, the control is designed based on back-stepping and sliding mode control. The control law design procedures are illustrated in the following steps.

Step1: Same procedures as explained in Step 1 of Section 3.3.1. The equivalent control for u_{1bsmc_dis} and u_{2bsmc_dis} are written in Equation (3-65) and (3-66) respectively.

$$u_{1bsmc\_eq} = \frac{1}{g_1}\{f_1(x,t) + g_1(x,t)\delta_1(x,t) + e_1 + K_{11bsmc}\dot{e}_1 + K_{12bsmc}s_{1bsmc} - \ddot{x}_{1d}\} \quad 3\text{-}65$$

$$u_{2bsmc\_eq} = -(K_{21bsmc}s_{2bsmc} + \delta_5(x,t) - \dot{x}_{7d}) \quad 3\text{-}66$$

Step 2: Define the discontinuous control, u_{1bsmc_dis} and u_{2bsmc_dis}

The reachability conditions of back-stepping SMC is defined based on conventional SMC. The reachability condition is written in Equations (**Error! Reference source not found.**) and (**Error! Reference source not found.**) respectively.

$$u_{1bsmc\_dis} = -M_1 sign(s_{1bsmc}) \quad 3\text{-}67$$

$$u_{2bsmc\_dis} = -M_2 sign(s_{2bsmc}) \quad 3\text{-}68$$

Finally the overall control law for back-stepping SMC is written in Equations (3-69) and (3-70) respectively

$$u_{1bsmc} = u_{1bsmc\_eq} + u_{1bsmc\_dis} = \frac{1}{g_1}\{f_1(x,t) + g_1(x,t)\delta_1(x,t) + e_1 + K_{11bsmc}\dot{e}_1 + K_{12bsmc}s_{1bsmc} - \ddot{x}_{1d}\} - M_1 sign(s_{1bsmc}) \quad 3\text{-}69$$

$$u_{2bsmc} = u_{2bsmc\_eq} + u_{2bsmc\_dis} = -(K_{21bsmc}s_{2bsmc} + \delta_5(x,t) - \dot{x}_{7d}) - M_2 sign(s_{2bsmc}) \quad 3\text{-}70$$

CHAPTER 4

RESULTS AND DISCUSSION

4.1 Introduction

In this chapter, the results and discussions of the research works are discussed and presented. The results will be discussed the tracking performance of the proposed controller. The tracking performance will be evaluated in terms of chattering reduction and steady state error.

4.2 Performance of back-stepping sliding mode control (BSTSMC)

The BSTSMC controller is an algorithm that combines two techniques which are the back-stepping control and STSMC. The integration of these two techniques has produced the controller with the advantage of back-stepping that is systematic and recursive methodology with asymptotically stability and STSMC ensures that the sliding surfaces are converged in finite time. The controller was designed for the nonlinear equations of an AUG longitudinal plane that has been presented in Chapter 3. The control system consists of two inputs and seven outputs. However in this study, there were only two outputs considered which were the pitching angle (θ) and net-buoyancy (m_{em}). The simulations were done using the parameters adopted from Graver, (2005) as depicted in Table 4-1

Table 4-1 Parameter values of the AUG

Parameter	Value	Unit
Hull mass, $\boldsymbol{m_h}$	40	kg
Internal sliding mass, $\boldsymbol{m_p}$	9	kg
Displaced fluid mass, $\boldsymbol{m_{df}}$	50	kg
Added mass, $\boldsymbol{m_{f1}, m_{f2}, m_{f3}}$	5, 60, 70	kg
Inertia, $\boldsymbol{J_1, J_2, J_3}$	4, 12, 11	kgm^2
Lift coefficient, $\boldsymbol{K_{LO}, K_L}$	0, 132.5	-
Drag coefficient, $\boldsymbol{K_{DO}, K_D}$	2.15, 25	-

Moment coefficient, $\boldsymbol{K_{MO}}, \boldsymbol{K_M}$	0, -100	-
Constant coefficient, $\boldsymbol{K_{\omega_2^1}}, \boldsymbol{K_{\omega_2^2}}$	50, 50	-

The proposed controller was developed and simulated using MATLAB™. The block diagram of a BSTSMC algorithm is shown in Figure 4-1. The simulations have been carried out for the glider to glide from -25° to 25°. The initial values of the states and desired observed outputs are depicted in Table 4-2. All the controller gains are heuristically tuned. The parameter p in continuous part of super twisting sliding mode in Equation (4.75) is chosen as 0.5 to ensure maximum real sliding order of super twisting realisation is achieved as suggested by various previous works (Bartolini et al., 1999; Arie Levant & Fridman, 2002; Arie Levant, 2007; Salgado-Jimenez & Jouvencel, 2003). The proposed controller parameter values are depicted in Table 4-3.

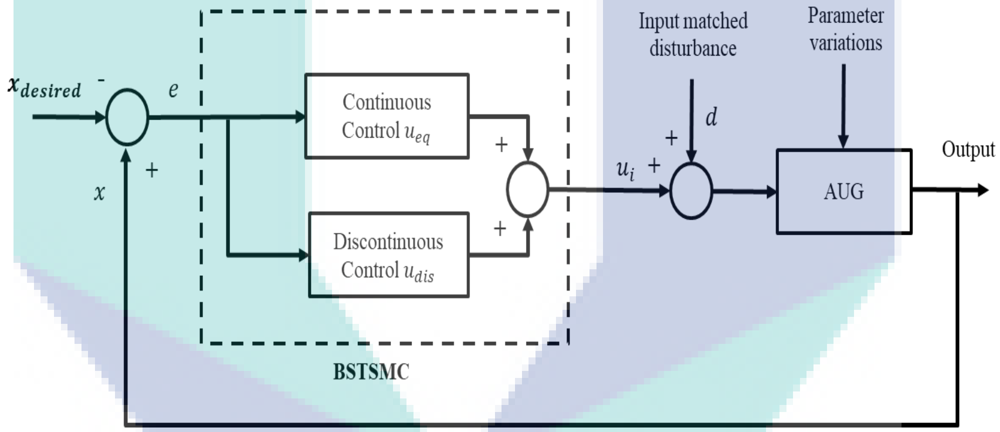

Figure 4-1 The block diagram of a BSTSMC

Table 4-2 The initial and desired values of the states

Parameter	Initial	Desired
Pitching angle, $\boldsymbol{\theta}$	-23°	23°
Surge velocity, $\boldsymbol{v_1}$	0.3 ms^{-1}	-
Heave velocity, $\boldsymbol{v_3}$	0.02 ms^{-1}	-
x- position of internal mass, $\boldsymbol{r_{p1}}$	1.98 cm	-
Ballast mass, $\boldsymbol{m_b}$	1.05 kg	0.95 kg
Excess mass, $\boldsymbol{m_{em}}$	0.05 kg	-0.05 kg

Table 4-3 The BSTSMC controller gains

Parameter	θ	m_{em}
	Nominal system	
Back-stepping gain	K_{11} = 0.90, K_{12} = 6.02	K_{21} = 25
Super twisting gain	β_{11} = 0.50, β_{12} = 0.01	β_{21} = 0.10 β_{22} = 0.001
	With disturbance	
Back-stepping gain	K_{11} = 0.20, K_{12} =30	K_{21} = 1450
Super twisting gain	β_{11} = 45, β_{12} = 30	β_{21} = 10, β_{22} = 1
	Parameter variation	
Back-stepping gain	K_{11} = 0.20, K_{12} =30	K_{21} = 1450
Super twisting gain	β_{11} = 45, β_{12} = 30	β_{21} = 10, β_{22} = 1

The BISTSMC was tested for the nominal system which is the system with presence of external disturbance and parameter variations. The responses of the observed outputs, control inputs and sliding surfaces are shown in Figure 4-2 to Figure 4-7. All cases are plotted on the same figures in order to evaluate the performance of the BSTSMC with and without perturbations.

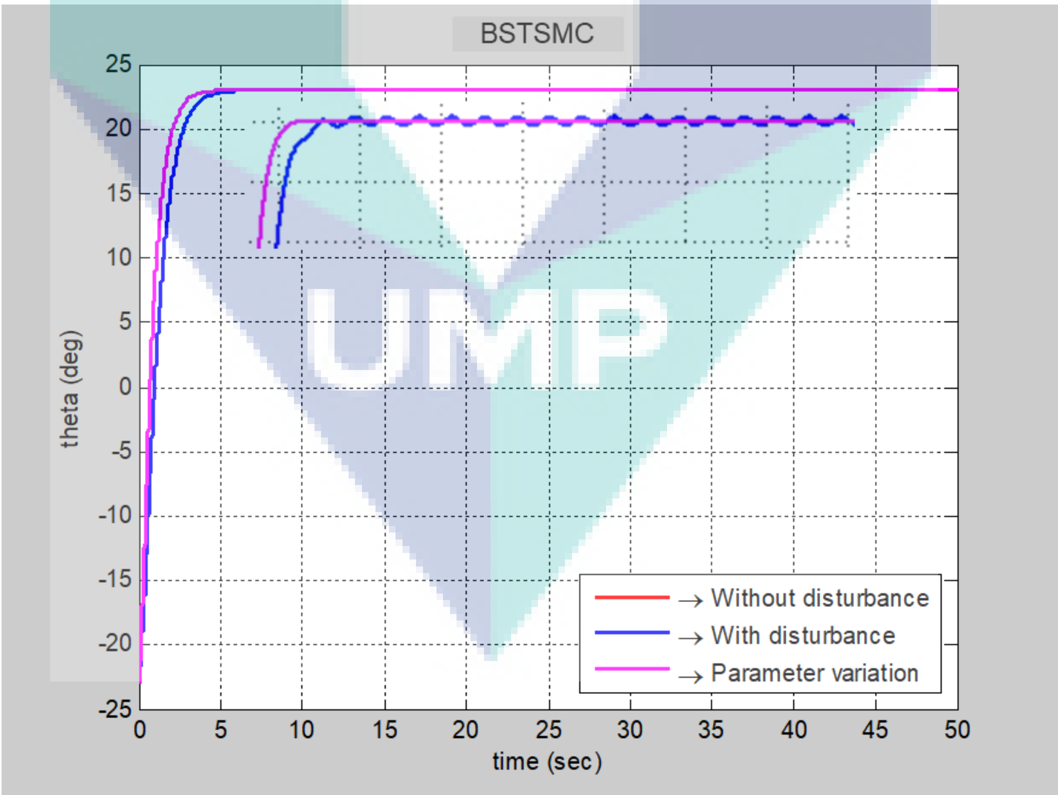

Figure 4-2 Pitching angle,θ (BSTSMC)

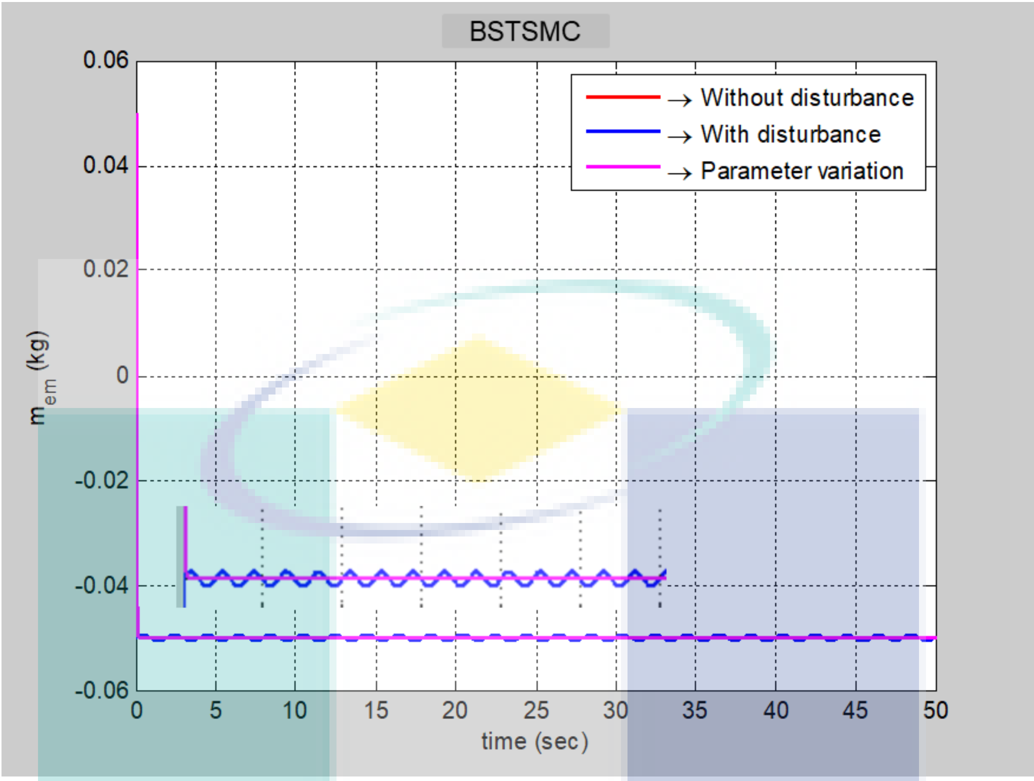

Figure 4-3 Net-buoyancy, m_{em} (BSTSMC)

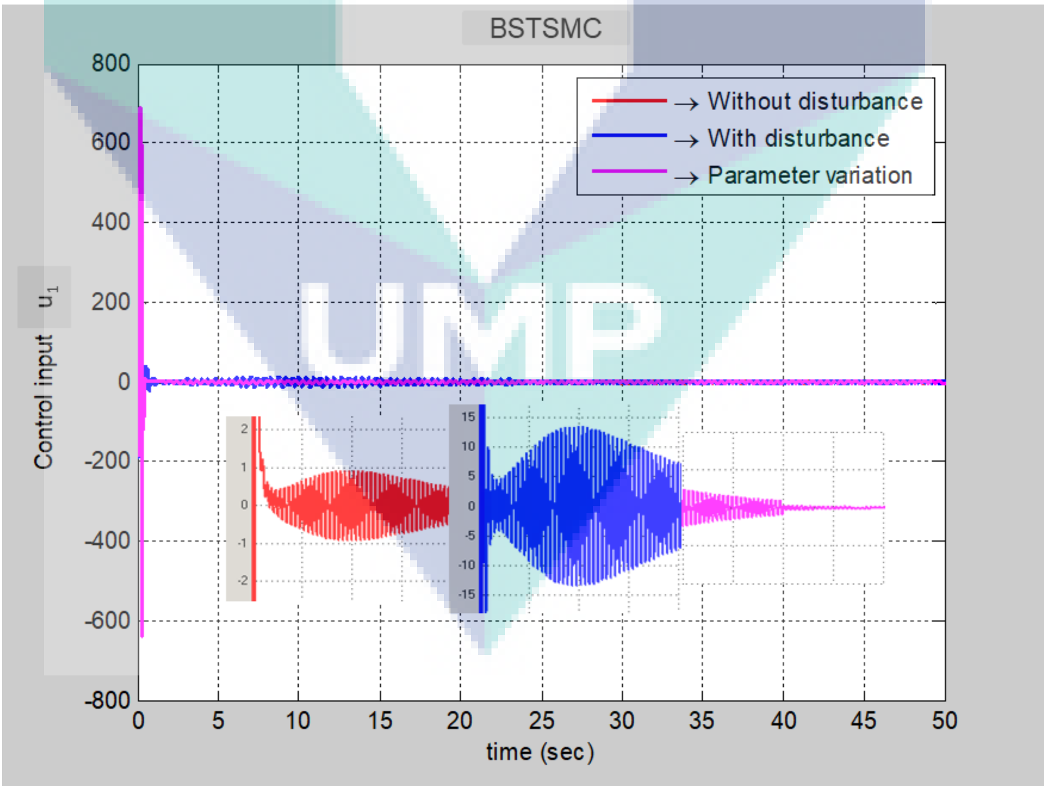

Figure 4-4 Control input, u_1 (BSTSMC)

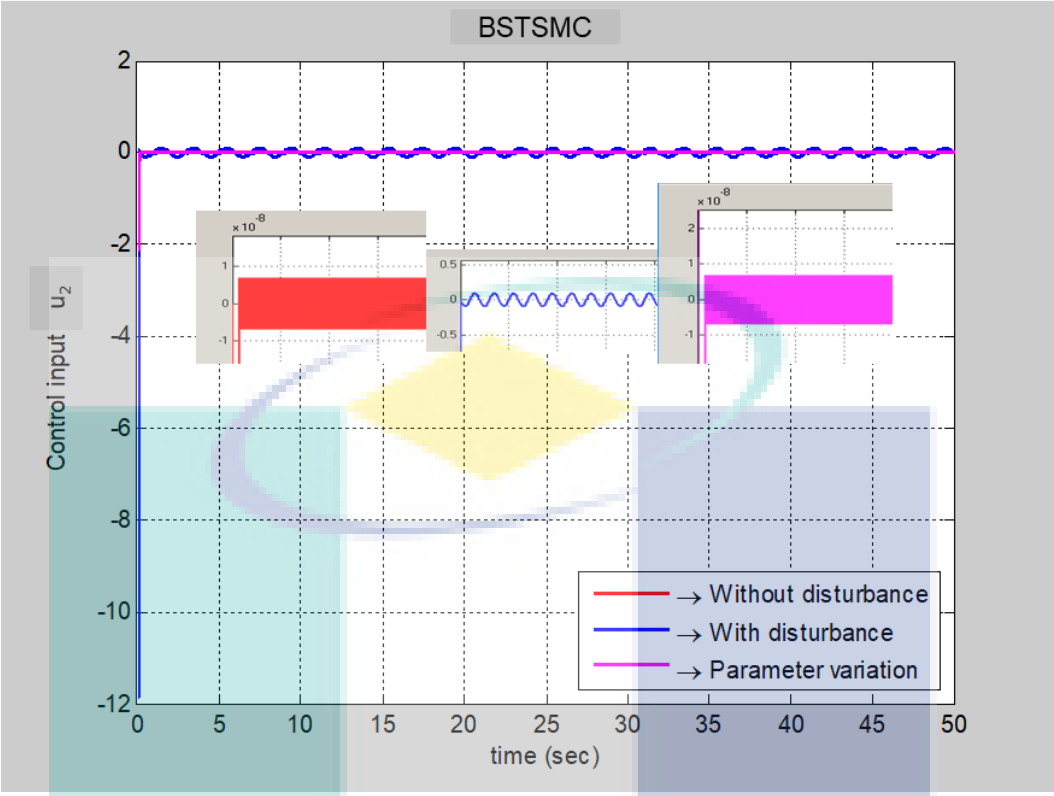

Figure 4-5 Control input, u_2 (BSTSMC)

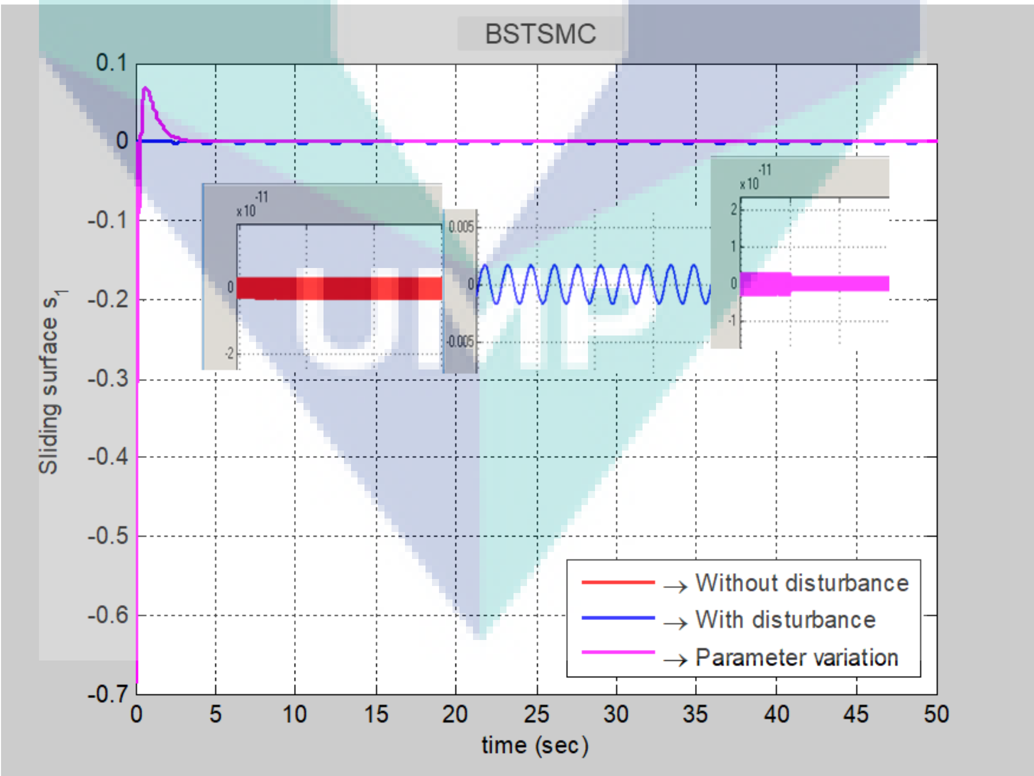

Figure 4-6 Sliding surface, s_1 (BSTSMC)

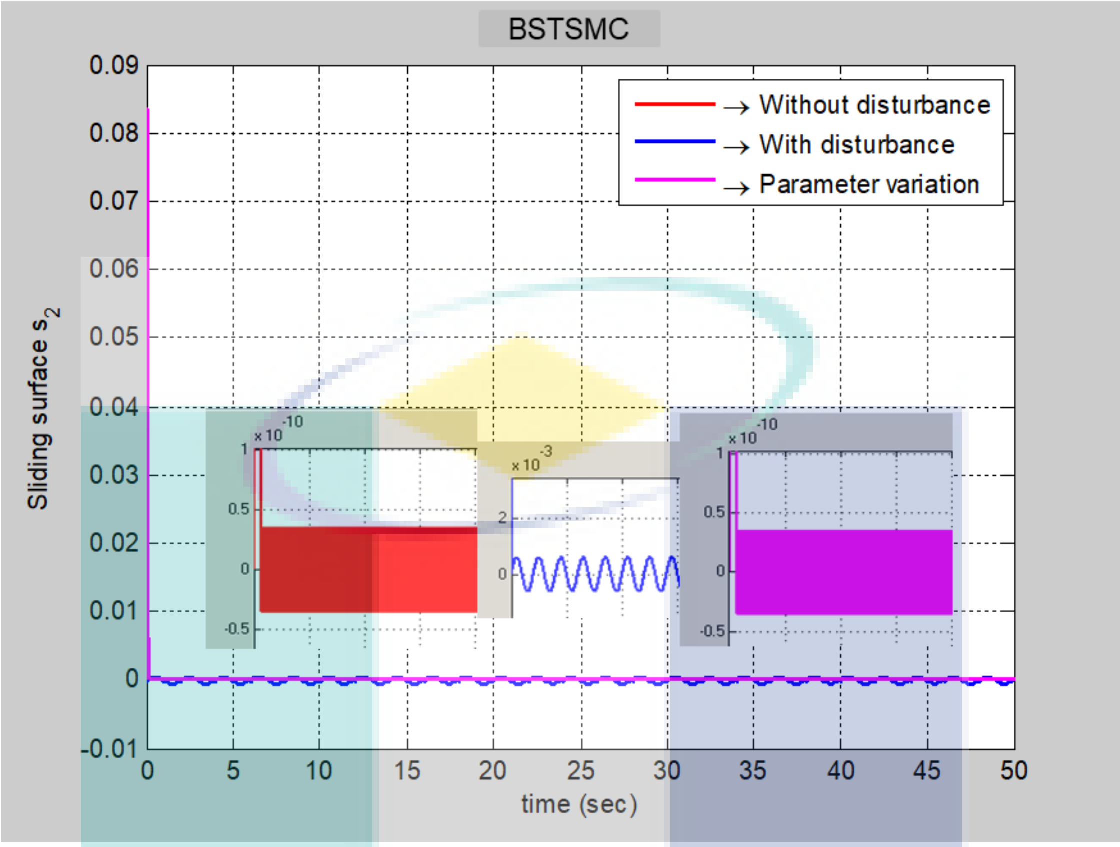

Figure 4-7 Sliding surface, s_2 (BSTSMC)

For the nominal system, the pitching angle is converged to desired value at about t = 7 seconds and net buoyancy at about t = 4 seconds with very small steady errors of 1.19 x 10-14° and 3.95 x 10-09kg for pitching angle and net buoyancy respectively. The control inputs are stabilised at about u_1 = 0.5 and u_2 = 6.83 x 10^{-9}. The sliding surfaces are stabilised in the vicinity of zero with s_1 = 3.17 x 10^{-12} and s_2 = 3.53 x 10^{-11}. The root mean square errors (RMSEs) for s_1 and s_2 are 3.17 x 10^{-12} and 3.53 x 10^{-11} respectively. The chattering is considered and eliminated because both control inputs and sliding surfaces do not show any chattering.

The inputs matched external disturbances of $\delta_1(x,t) = 5x_1\sin(\pi t)$ and $\delta_5(x,t) = 0.1x_7\sin(\pi t)$ are induced to input channels 1 and 2 respectively. Both disturbances are induced at $t = 0$. In real environment, water current gives a high impact on manoeuvrability of the AUG. Statnikov (2002) reported the speed of the water current did vary from 0.02 ms^{-1} to 2.5 ms^{-1}. Therefore, the selected disturbances for the simulations are considered to be practical. The proposed algorithm is able to stabilise the observed outputs in the vicinity of the desired values with RMSE about 1.35 x 10^{-04}° for pitching angle and 1.98 x 10^{-06}kg for net buoyancy. The control input

u_1 is reduced from 0.5 to 0.07, however control input u_2 is increased from 6.83 x 10^{-09} to 1.71 x 10^{-03}. Both RMSEs of sliding surfaces are increased from 3.17 x 10^{-12} to 3.97 x 10^{-06} for s_1 and from 3.53 x 10^{-12} to 1.98 x 10^{-06} for s_2. The simulation results have shown that the proposed controller is able to stabilise the outputs to the desired values with considerably low errors. The chattering is considered to be eliminated with small oscillations.

The BSTSMC has also been tested for parameter variations. The hydrodynamics coefficients, added mass and inertia of AUG have shown to increase by 30%. Table 4-4 shows the nominal values and increased values of the parameters. The increment is applied to the system starting from $t = 25$ seconds. The simulations have shown that the outputs are able to converge to the desired values in about 7 seconds for pitching angle and about 4 seconds for net buoyancy. The RMSE for pitching angle is 6.88 x 10^{-15}° and net buoyancy is 3.95 x 10^{-09}kg. The proposed controller is able to achieve the performance of the nominal system. The control effort u_1 is reduced from 0.5 to 0.003 and u_2 is consistent at about the same as the nominal system. The RMSE of sliding s_1 is reduced about 40% and s_2 is retained the same RMSE value. The proposed controller is able to suppress the chattering even after parameter variations are imposed to the aforementioned parameters.

From the results, the proposed controller is able to suppress the chattering in all cases, thus proving that the proposed controller is robust against external disturbance and parameter variations.

Table 4-4 Increment of parameters

Parameter	Nominal	Increased (30%)
m_{f1}	5 kg	6.5 kg
m_{f3}	70 kg	91 kg
J_2	12 kgm^2	15.60 kgm^2
K_{LO}	0	0.30
K_L	132.5	172.25
K_{DO}	0, 132.5	-
K_D	2.15, 25	-
K_{MO}	0, -100	-
K_M		

$\boldsymbol{K_{\omega_2^1}, K_{\omega_2^2}}$	50, 50	-

4.3 Controller benchmarking

This section presents the results and discussion for performance benchmarking of the proposed nonlinear (BSTSMC) controllers. The performance of the nonlinear proposed controller is benchmarked with combination of back-stepping and SMC control strategies which are STSMC and back-stepping SMC. The performance is analysed in terms of steady-state error, control effort and chattering reduction.

The same AUG parameters from Section 4.2, Table 4-1 and Table 4-2 are used for the simulations in this section. The performance is evaluated for nominal system, system with induced disturbance and system with parameter variations.

The responses of the observed outputs, control inputs and sliding surfaces for the nominal system are shown in Figure 4-8 to Figure 4-13. All the controllers are able to be stabilised at the desired value with very small steady-state error. Figure 4-8 and Figure 4-9 show that the STSMC gives the largest value of RMSE of 4.39 x 10^{-09}° for pitching angle and 2.59 x 10^{-05} kg for net buoyancy. The back-stepping ISMC shows the RMSE value of 4.05 x 10^{-09}° and 1.05 x 10^{-07} kg for net buoyancy and back-stepping STSMC shows RMSE value of 2.62 x 10^{-10}° for pitching angle and 1.14 x 10^{-07} kg for net buoyancy. BSTSMC provides the smallest RMSE value of 1.19 x $10^{-14°}$ for pitching angle and 3.95 x 10^{-09} kg for net buoyancy.

Figure 4-10 and Figure 4-11 show the responses for control inputs. The control inputs of all controllers are stabilised in the vicinity of zero. The STSMC shows largest control effort for u_1 of about 0.63 and for u_2 of about (4.53 x 10^{-3}). The smallest control effort for u_2 is given by the proposed controller which is 6.83 x 10^{-09}.

From Figure 4-12 and Figure 4-13, the sliding surfaces of all controllers are converged to origin. The proposed controller gives the smallest RMSE value for both sliding surfaces with value 3.17 x 10^{-12} for s_1 and 3.53 x 10^{-11} for s_2. All benchmarked controllers demonstrate very small chattering however, STSMC shows the largest chattering. The proposed control successfully suppresses the chattering with no oscillation.

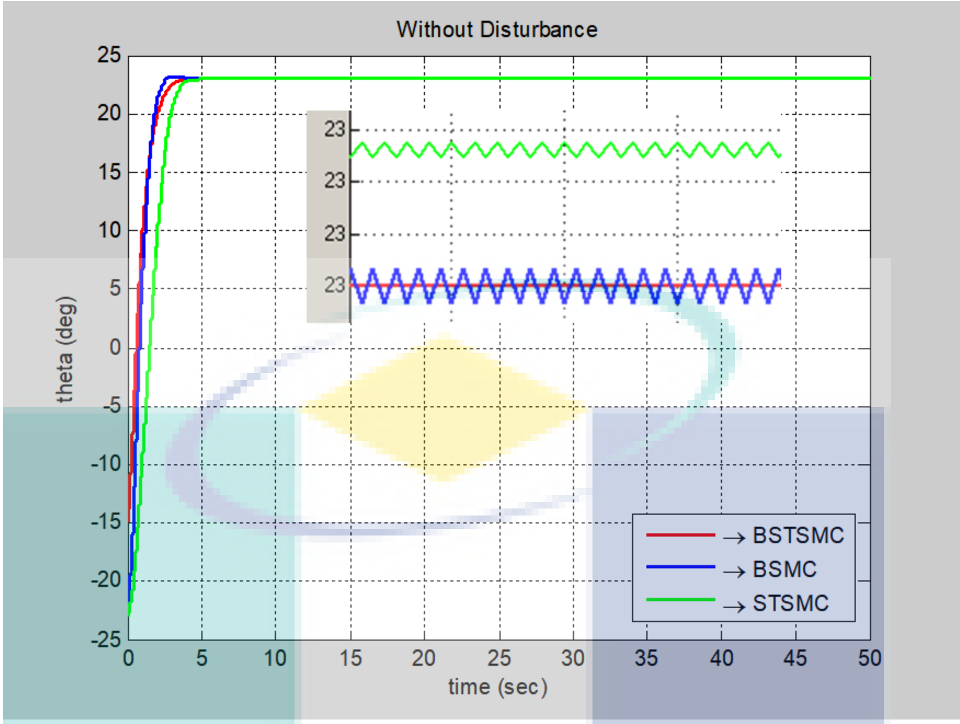

Figure 4-8 Pitching angle, θ(without disturbance)

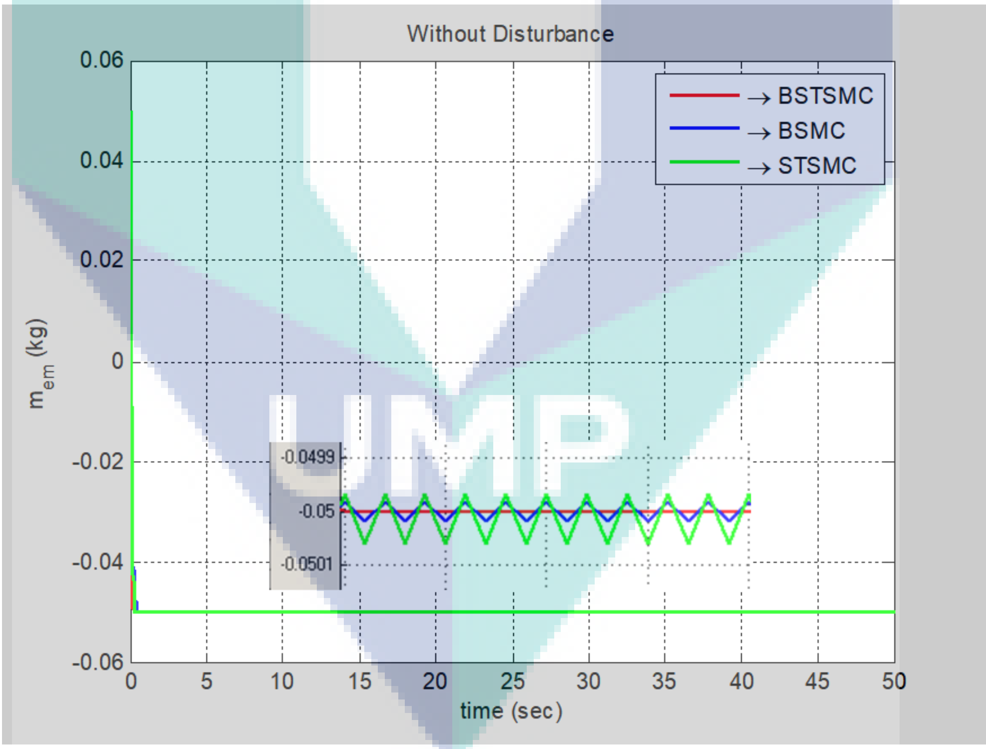

Figure 4-9 Net buoyancy, m_{em} (without disturbance)

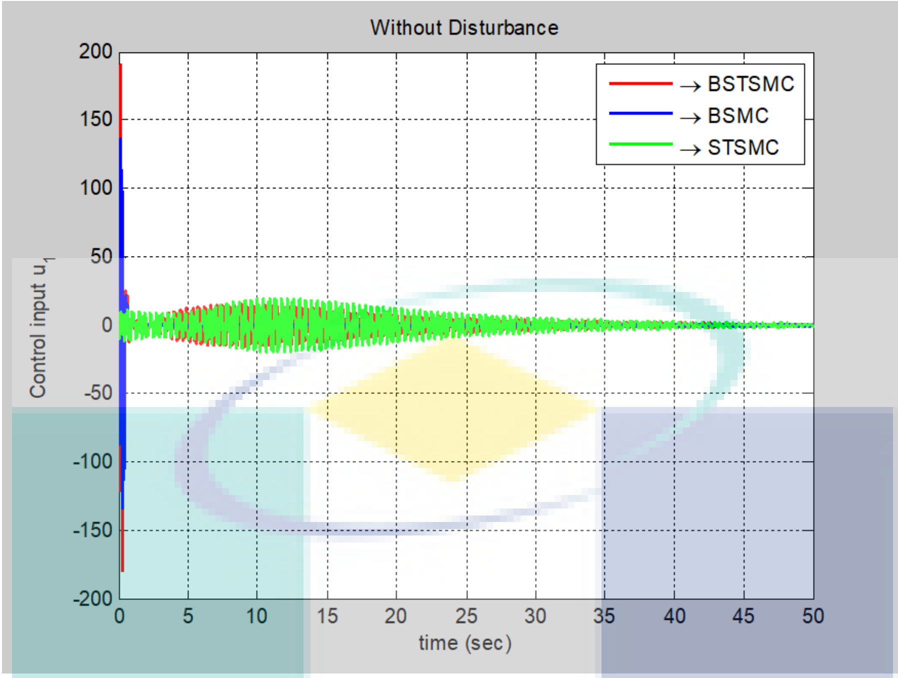

Figure 4-10 Control input, u_1 (without disturbance)

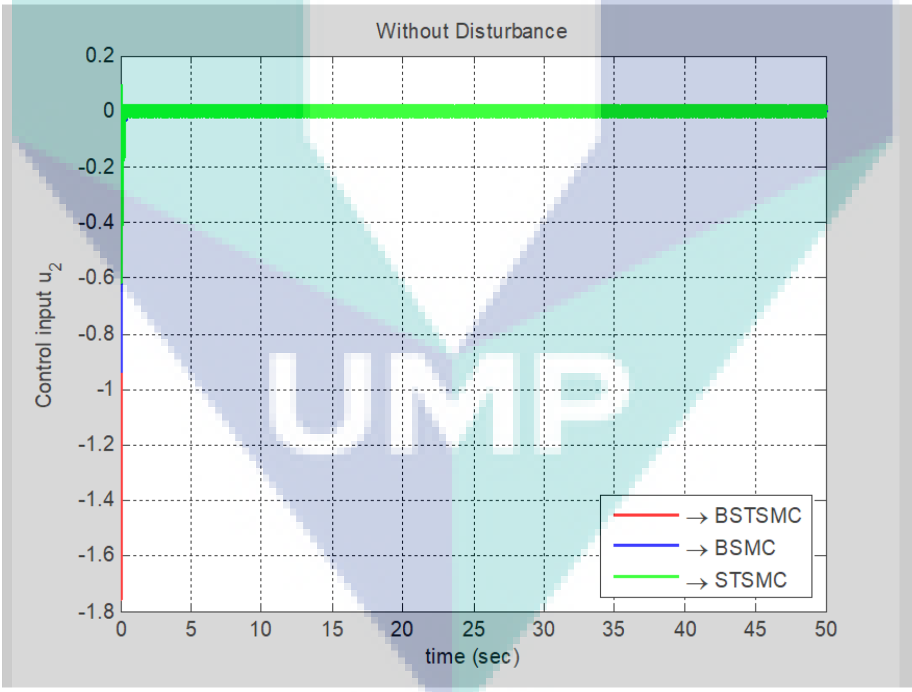

Figure 4-11 Control input, u_2 (without disturbance)

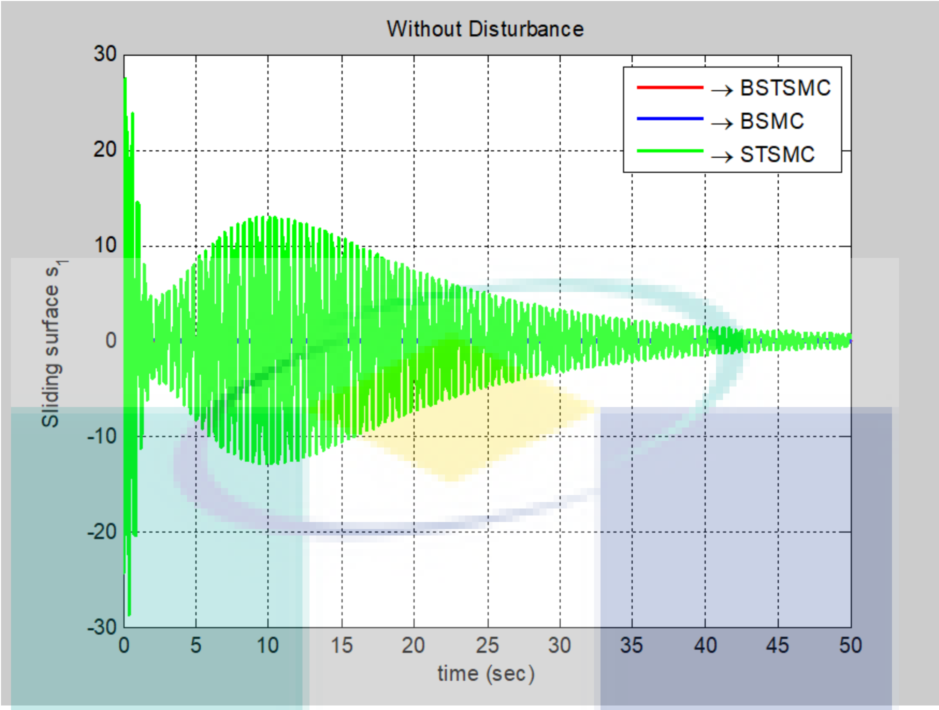

Figure 4-12 Sliding surface, s_1 (without disturbance)

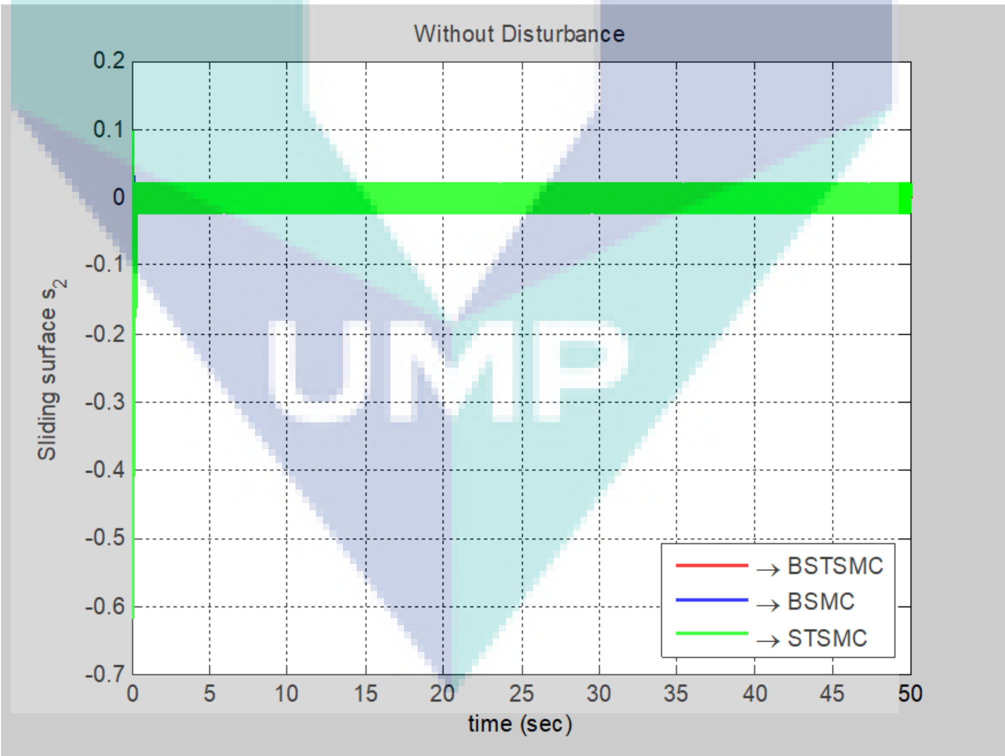

Figure 4-13 Sliding surface, s_2 (without disturbance)

The same disturbances in Section 4.2 have been induced to the system to evaluate the performance of the proposed controller algorithm against STSMC, back-stepping and back-stepping SMC. The responses for the system with induced disturbance are shown in Figure 4-14 to Figure 4-19. From Figure 4-14 and Figure 4-15, all controllers are able to be stabilised in the vicinity of the desired values with increment in steady-state errors. The STSMC shows the largest steady-state error for pitching angle with RMSE value of 5.82 x 10^{-06}° and for net buoyancy with RMSE value of 8.61 x 10^{-05}kg. The proposed controller provides the smallest steady-state error with the smallest oscillation for both outputs.

Figure 4-16 and Figure 4-17 show the control effort u_1 of is increasing while the control effort u_1 for the proposed controller is decreasing. However, all controllers show increment in the control effort u_2 with STSMC that gives the highest control effort with magnitude of 0.08 and the proposed controller shows the smallest effort with magnitude of 2.13 x 10^{-03} and back-stepping SMC is 1.34 x 10^{-02}. The sliding surface of all controllers are converged to the vicinity of origin with the proposed controller yields the smallest RMSE value as shown in Figure 4-18 and Figure 4-19. From the results, the proposed controller shows the smallest chattering and smallest steady-state error.

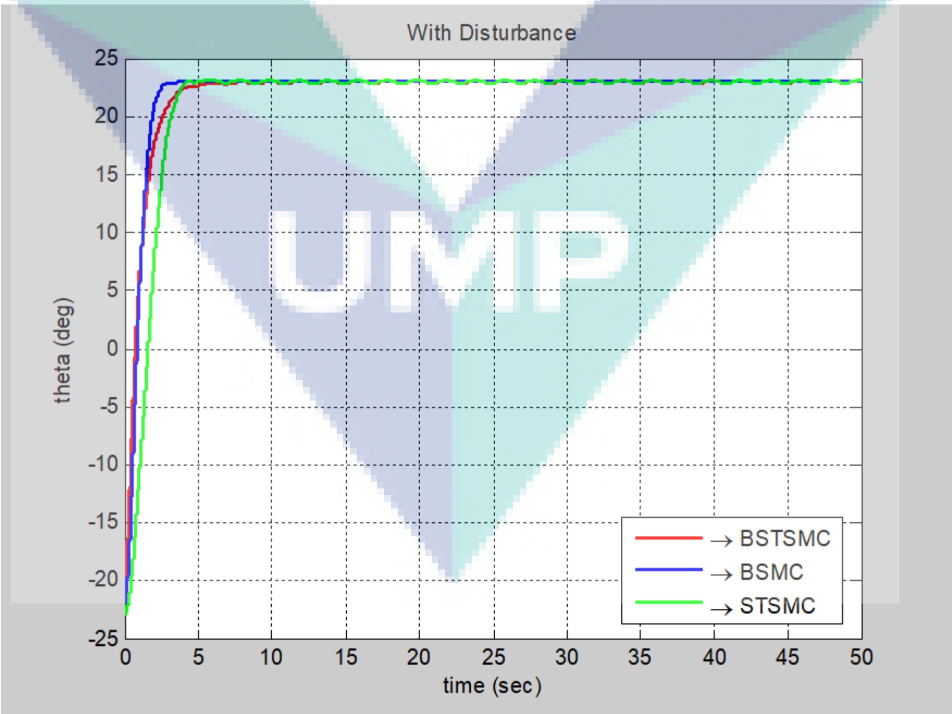

Figure 4-14 Pitching angle, θ(with disturbance)

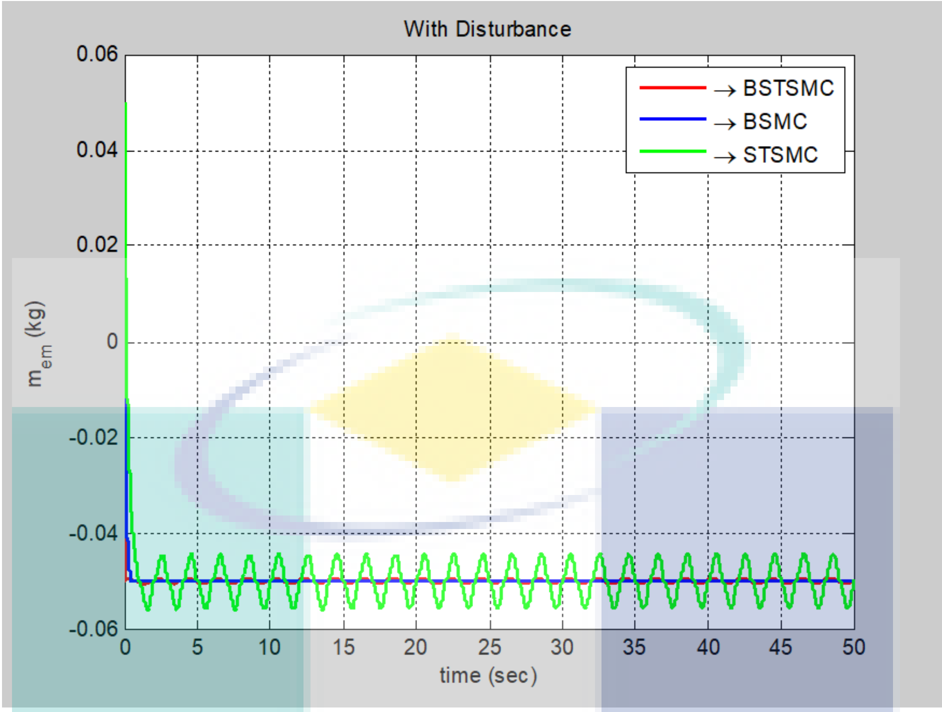

Figure 4-15 Net buoyancy, m_{em} (with disturbance)

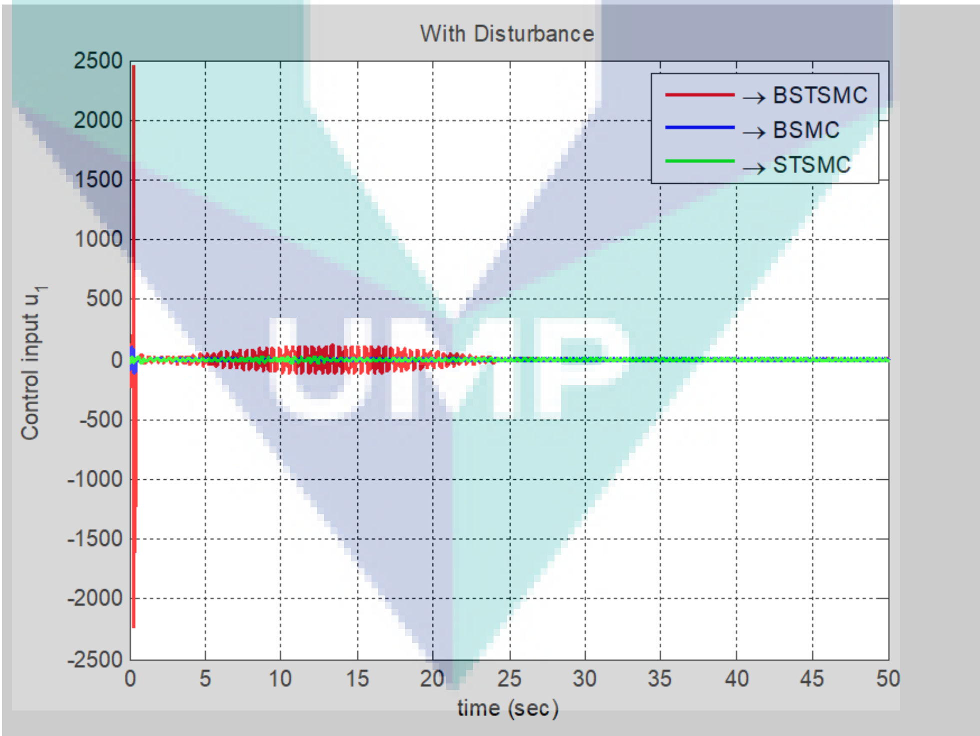

Figure 4-16 Control input, u_1 (with disturbance)

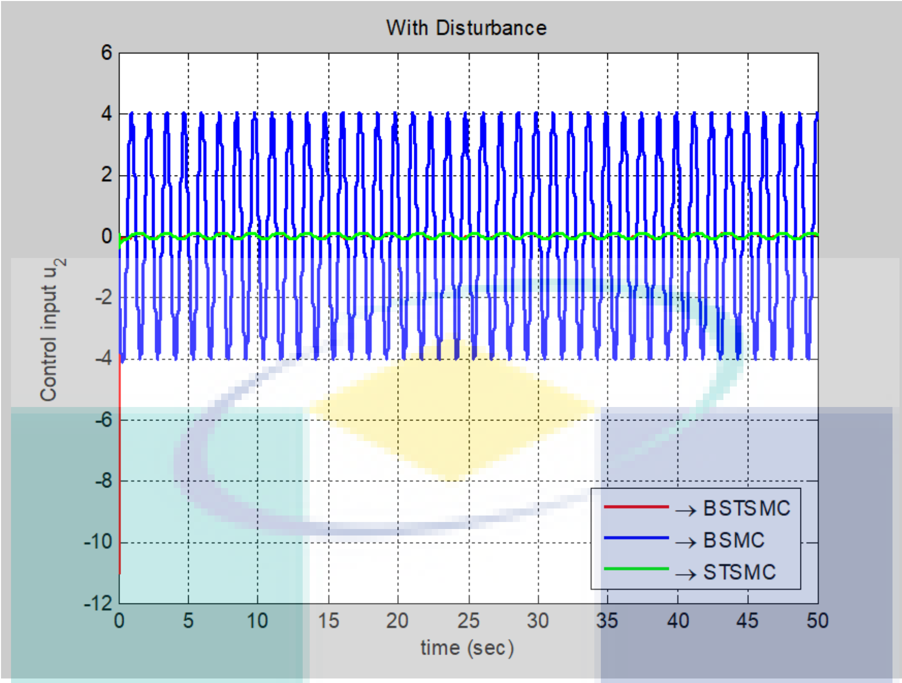

Figure 4-17 Control input, u_2 (with disturbance)

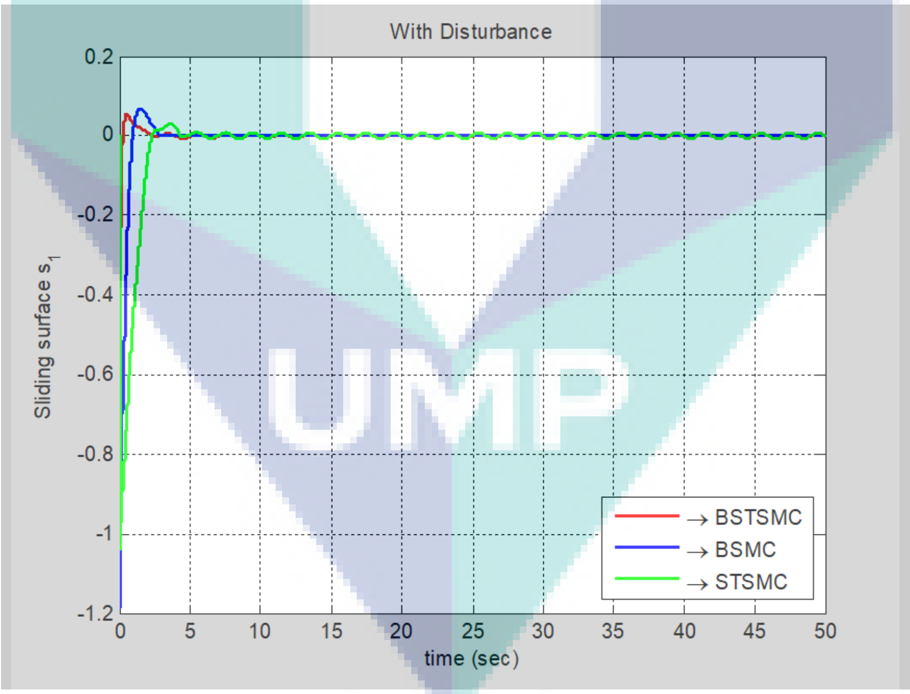

Figure 4-18 Sliding surface, s_1 (with disturbance)

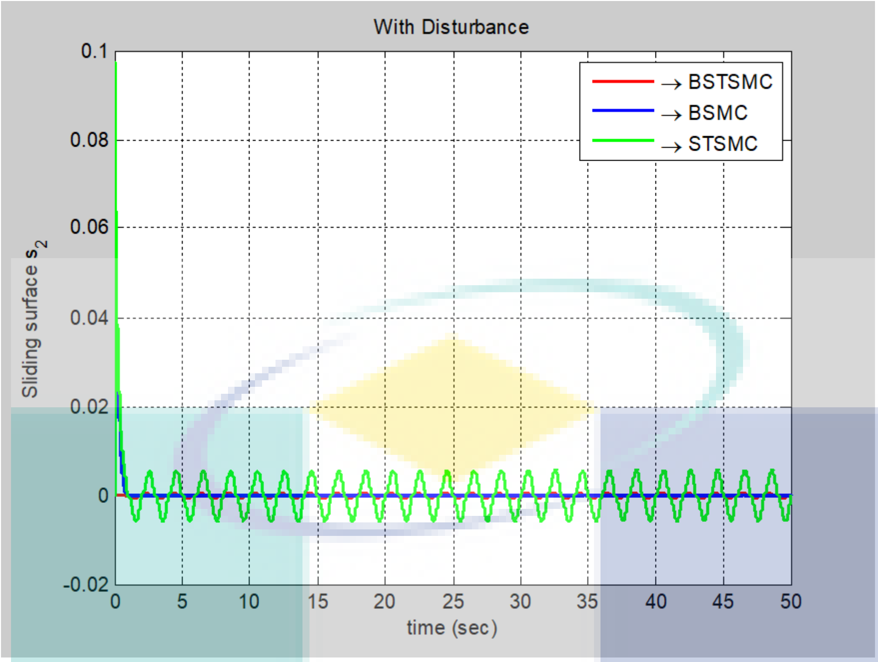

Figure 4-19 Sliding surface, s_2 (with disturbance)

The same increment of parameters in Section 4.2 has been used for evaluating the performance of the proposed controller algorithm against the performance of ISTSMC, back-stepping ISMC and back-stepping STSMC. Figure 4-20 to Figure 4-25 show the responses for the parameter variations. From Figure 4-20, it can be clearly seen that the proposed controller is not affected by the variation with the proposed controller which shows the highest accuracy. The STSMC shows the largest 'spike' at t = 25 and it takes There is no significant effects on the net buoyancy is observed here. All controllers are able to maintain their performances with the proposed controller showing the smallest RMSE value of 6.88 x 10^{-15}° for pitching angle and 3.95 x 10^{-09}kg for net buoyancy. The STSMC provides the largest RMSE value of 4.33 x 10^{-09}° for pitching angle and 2.56 x 10^{-05}kg for net buoyancy. The magnitude of control efforts and sliding surfaces of all controllers decreases.

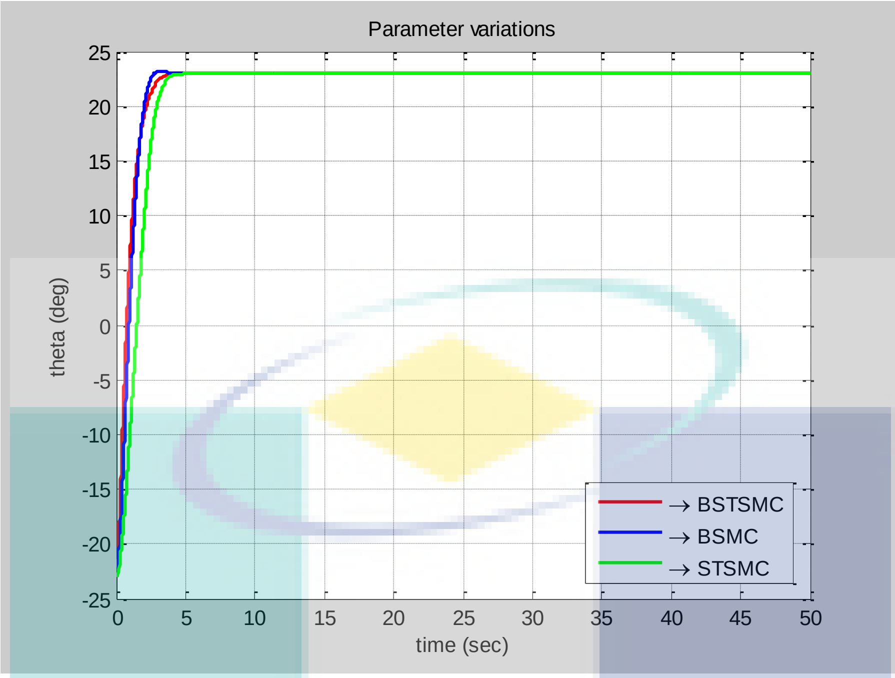

Figure 4-20 Pitching angle, θ (parameter variations)

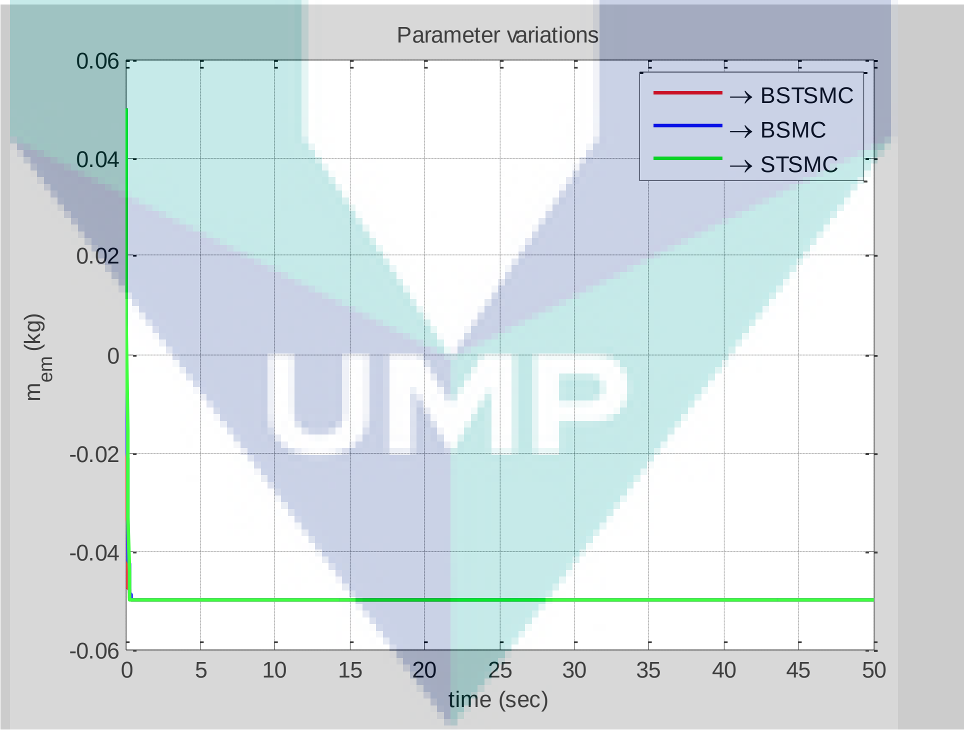

Figure 4-21 Net buoyancy, m_{em} (parameter variations)

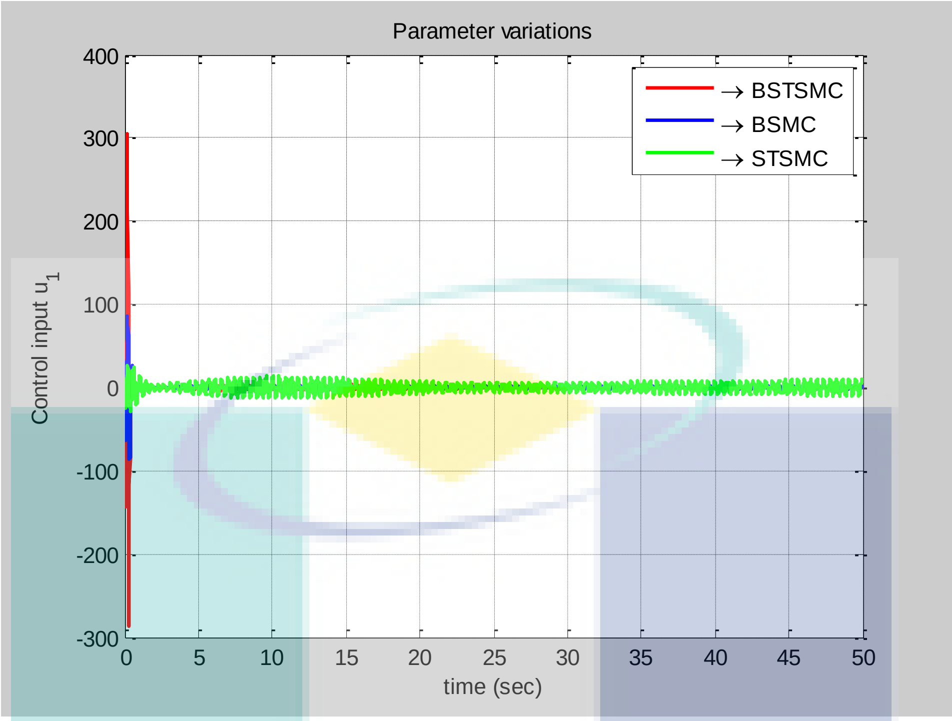

Figure 4-22 Control input, u_1(parameter variations)

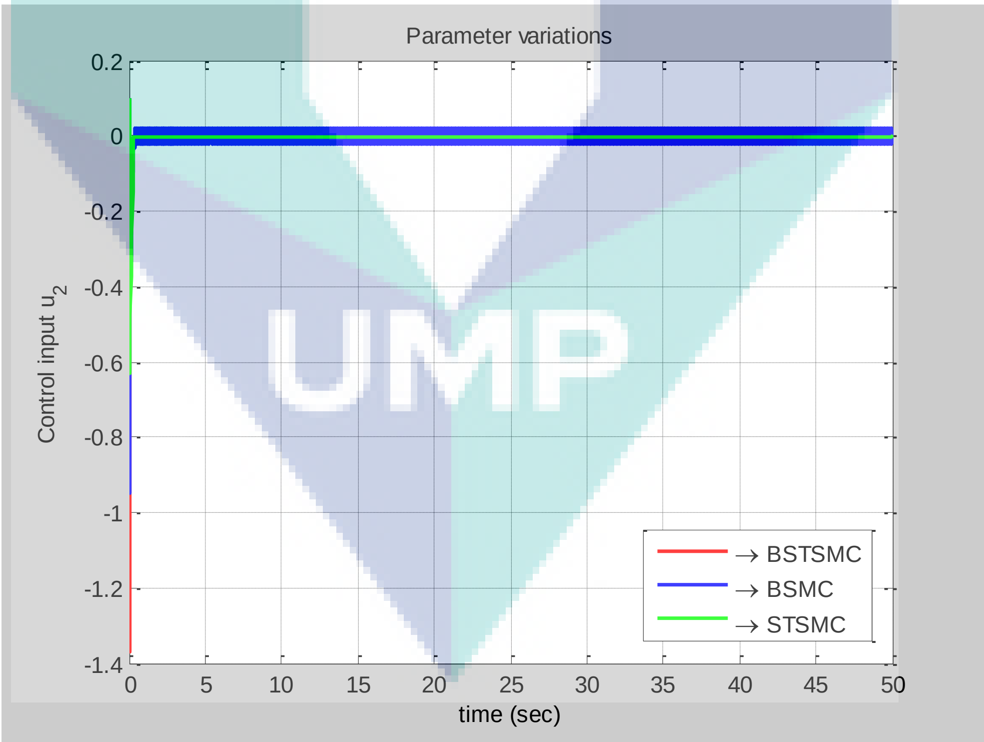

Figure 4-23 Control input, u_2 (parameter variations)

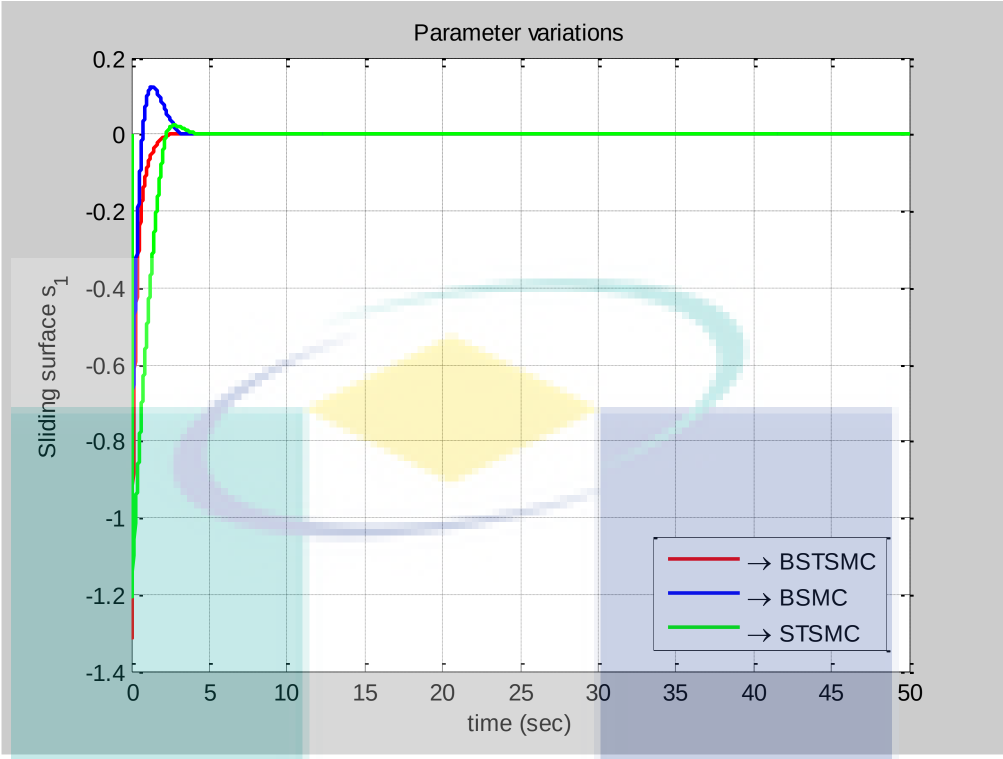

Figure 4-24 Sliding surface, s_1 (parameter variations)

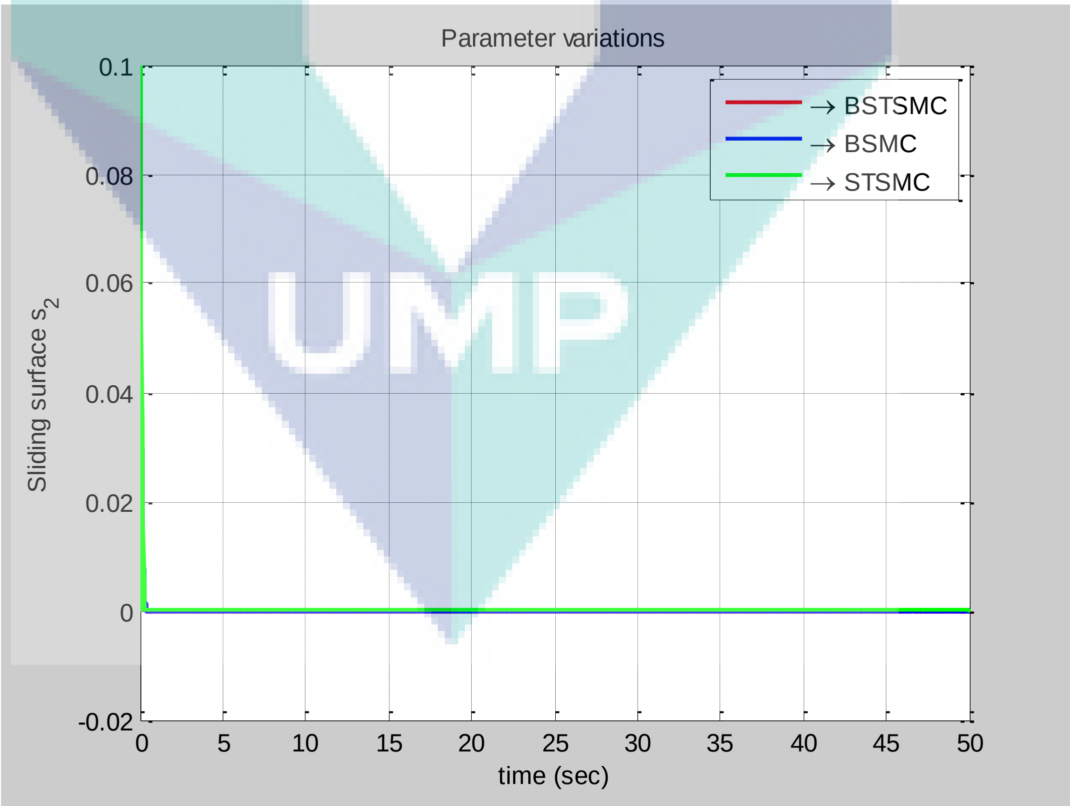

Figure 4-25 Sliding surface, s_2 (parameter variations)

CHAPTER 5

CONCLUSION

5.1 Conclusion

In this research work, three objectives have been set in Chapter 1. After completing all the works, all three objectives have been fulfilled. The BSTSMC was proposed for the nonlinear model. The BSTSMC was designed by combining two control strategies which are back-stepping and STSMC. The proposed controller has gained the advantage of every strategy. The back-stepping is known as a recursive methodology to obtain asymptotic stability via Lyapunov theorem and the super twisting SMC ensures the sliding surface to be converged in a finite time. The BSTSMC was designed and tested in the presence external disturbance as well as parameter variations. The performance of the BSTSMC was compared its performance against back-stepping SMC and STSMC. From the comparison, BSTSMC had demonstrated the highest performance as compared to back-stepping SMC and STSMC.

5.2 Recommendation

From the results and conclusions, improvements can be made to improve the performance of the proposed controllers. Therefore, several recommendations can be imposed for future works.

The first improvement is to optimise parameters of the controller. The optimisation can be done using any optimisation methods such as particle swarm optimisation, simulated Kalman filter and other available optimisation methods. In addition, various performance comparisons can be made with different optimisation methods to obtain the most optimised parameters of the controller. Secondly, the adaptive control can also be included in the proposed controller algorithm so that the controller has the adaptability to the disturbance of any other perturbations imposed to the system. An observation based on controller can also be used so that with estimated states, it can reduce the control effort and chattering further.

REFERENCES

Bartolini, G., Ferrara, A., Levant, A., & Usai, E. (1999). On Second Order Sliding Mode Controllers. *Variable structure systems, sliding mode and nonlinear control*, *247*, 329–350.

Budiyono, A. (2009). Advances in unmanned underwater vehicles technologies : Modeling , control and guidance perspectives. *Indian Journal of Geo-Marine Sciences*, *38*(3), 282–295.

Burlion, L., Ahmed-Ali, T., & Seube, N. (2004). Glider's roll control based on back-stepping. *IFAC Proceedings Volumes*, *37*(10), 161–165. Elsevier.

Caiti, A., Calabrò, V., Geluardi, S., Grammatico, S., & Munafò, A. (2012). Switching control of an underwater glider with independently controllable wings. *IFAC Proceedings Volumes*, *45*(27), 194–199.

Cao, J., Cao, J., Zeng, Z., & Lian, L. (2016). Nonlinear multiple-input-multiple-output adaptive back-stepping control of underwater glider systems. *International Journal of Advanced Robotic Systems*, *13*(6), 1–14.

Cao, Jun liang, Yao, B. heng, & Lian, L. (2015). Nonlinear pitch control of an underwater glider based on adaptive back-stepping approach. *Journal of Shanghai Jiaotong University (Science)*, *20*(6), 729–734.

Dougherty, F., Sherman, T., Woolweaver, G., & Lovell, G. (1988). An autonomous underwater vehicle (AUV) flight control system using sliding mode control. *OCEANS '88. A Partnership of Marine Interests. Proceedings* (pp. 1265–1270 vol.4).

Eriksen, C. C., Osse, T. J., Light, R. D., Wen, T., Lehman, T. W., Sabin, P. L., Ballard, J. W., et al. (2001). Seaglider: a long-range autonomous underwater vehicle for oceanographic research. *IEEE Journal of Oceanic Engineering*, *26*(4), 424–436.

Graver, J. G. (2005). *Underwater Gliders: Dynamics, Control and Design*. Princeton University.

Graver, J., Liu, J., Woolsey, C., & Leonard, N. E. (1998). Design and Analysis of an Underwater Vehicle for Controlled Gliding. *32nd Conference on Information Scinces and Systems* (pp. 801–806). Princeton, USA.

Healey, A. J., & Lienard, D. (1993). Multivariable sliding mode control for autonomous diving and steering of unmanned underwater vehicles. *Oceanic Engineering, IEEE Journal of*, *18*(3), 327–339.

Heng, C. T., Jamaludin, Z., Hashim, A. Y. B., Abdullah, L., & Rafan, N. A. (2017). Design of super twisting algorithm for chattering suppression in machine tools. *International Journal of Control, Automation and Systems*, *15*(3), 1259–1266.

Isa, K. (2015). *Homeostatic Inspired Controller Algorithm for a Hybrid-driven Autonomous Underwater Glider*. Universiti Sains Malaysia.

Ismail, R. M. T. R., That, N. D., & Ha, Q. P. (2015). Automation in Construction Modelling and robust trajectory following for offshore container crane systems. *Automation in Contruction*, *59*, 179–187.

Jalani, J., Herrmann, G., & Melhuish, C. (2010). Robust Trajectory Following for Underactuated Robot Fingers. *UKACC International Conference on Control 2010* (pp. 1–6). Conventry, UK.

Kim, M., Joe, H., Kim, J., & Yu, S. (2015). Integral sliding mode controller for precise manoeuvring of autonomous underwater vehicle in the presence of unknown environmental disturbances. *International Journal of Control*, *88*(March 2015), 1–43. Taylor & Francis.

Leonard, N. E., & Graver, J. (2001). Model-based feedback control of autonomous underwater gliders. *IEEE Journal of Oceanic Engineering*, *26*(4), 633–645.

Levant, A. (1993). Sliding order and sliding accuracy in sliding mode control. *International Journal of Control*, *58*(6), 1247–1263.

Levant, A. (2007). Principles of 2-sliding mode design. *Automatica*, *43*(4), 576–586.

Levant, A., & Fridman, F. (2002). Higher Order Sliding Modes. In W. Perruquetti & J. P. Barbot (Eds.), *Sliding Mode Control in Engineering* (pp. 53–102). Taylor & Francis.

Li, S., Member, S., Zhou, M., & Yu, X. (2013). Design and implementation of terminal sliding mode control method for PMSM speed regulation system. *IEEE Transactions on Industrial Informatics*, *9*(4), 1879–1891.

Mat-Noh, M., Mohd-Mokhtar, R., Arshad, M. R., Zain, Z. M., & Khan, Q. (2019). Review of sliding mode control application in autonomous underwater vehicles. *Indian Journal of Geo-Marine Sciences*, *48*(7), 973–984.

Md Zain, Z. (2012). *Underactuated Control for an Autonomous Underwater Vehicle with Four Thrusters*. Okayama University, Okayama, Japan.

Rhif, A. (2012). Stabilizing sliding mode control design and application for DC motor: speed control. *International Journal of Instrumentation and Control Systems (IJICS)*, *2*(1), 39–

48.

Salgado-Jimenez, T., & Jouvencel, B. (2003). Using a high order sliding modes for diving control a torpedo autonomous underwater vehicle. *Oceans 2003* (pp. 934–939). San diego, USA.

Sherman, J., Davis, R. E., Owens, W. B., & Valdes, J. (2001). The autonomous underwater glider "Spray." *IEEE Journal of Oceanic Engineering*, *26*(4), 437–446.

Tayebi-haghighi, S. (2018). Robust Composite High-Order Super-Twisting. *Robotics*, *7*(1), 1–18.

Wang, L., Liu, J., Yu, H., & Xu, Y. (2002). Sliding Mode Control of an Autonomous Underwater Vehicle. *Proceeding of the First International Conference on Machine Learning and Cybernetics* (pp. 247–251).

Webb, D. C., Simonetti, P. J., & Jones, C. P. (2001). SLOCUM: an underwater glider propelled by environmental energy. *IEEE Journal of Oceanic Engineering*, *26*(4), 447–452. Retrieved from http://ieeexplore.ieee.org/lpdocs/epic03/wrapper.htm?arnumber=972077

Yoerger, D. R., & Slotine, J.-J. . (1985). Robust trajectory control of underwater vehicles. *IEEE Journal of Oceanic Engineering*, *10*(4), 462–470.

Yuh, J. (2000). Design and Control of Autonomous Underwater Robots : A Survey. *Autonomous Robots, Kluwer Academic Publishers*, *8*(1), 7–24.

Zhao, S., & Yuh, J. (2005). Experimental Study on Advanced Underwater Robot Control. *Robotics, IEEE Transactions on*, *21*(4), 695–703.

LIST OF PUBLICATIONS

Journal

1. Mat-Noh, M., Mohd-Mokhtar, R., Arshad, M. R., Zain, Z. M., & Khan, Q. (2019). Review of sliding mode control application in autonomous underwater vehicles. Indian Journal of Geo-Marine Sciences, 48(7), 973–984.

Book Series

1. Mat-Noh, M., Arshad, M. R., Mohd-Mokhtar, R., Md Zain, Z., Khan, Q., & Abdul Kadir, H. (2019). Robust controller design for autonomous underwater glider using back-stepping super twisting sliding mode control algorithm. In Z. Md Zain, H. Ahmad, D. Pebrianti, M. Mustafa, N. R. H. Abdullah, R. Samad, & M. Mat Noh (Eds.), Proceedings of 10th National Technical Seminar on Underwater System Technology 2018 (NUSYS'18, 79–97. Springer Singapore. Scopus

2. Mat-Noh, M., Arshad, M. R., Mohd-Mokhtar, R., Md Zain, Z., & Khan, Q. (2018). Integral Super Twisting Sliding Mode Control (ISTSMC) Application in 1DOF Internal Mass Autonomous Underwater Glider (AUG). In M. Hassan (Ed.), Intelligent Manufacturing & Mechatronics, 305-325. Springer, Singapore. Scopus

Conference

1. Mat-Noh, M., Arshad, M. R., Mohd-Mokhtar, R., Khan, Q. (2017). Back-Stepping Sliding Mode Control Strategy for Autonomous Underwater Glider, in Proceedings of 2017 13th International Conference on Emerging Technologies (ICET) (pp. 1-6). Islamabad, Pakistan.(Scopus)

2. Mat-Noh, M., Arshad, M. R., Mohd-Mokhtar, R. (2017). Nonlinear Control of Autonomous Underwater Glider Based on Super twisting Sliding Mode Control (STSMC), 2017 7th IEEE International Conference on System Engineering and Technology (ICSET) (pp. 71-76). Shah Alam, Malaysia. (Scopus)